Design of On-demand DBS in Movement Disorders using Machine Learning and the Need for Adaptive Learning

BY

NIVEDITA KHOBRAGADE
M.S., Bioengineering, University of Texas at Arlington, 2012

THESIS

Submitted as partial fulfillment of the requirements
for the degree of Doctor of Philosophy in Electrical and Computer Engineering
in the Graduate College of the
University of Illinois at Chicago, 2019

Chicago, Illinois

Dissertation Committee:

Daniela Tuninetti, Chair and Advisor
Daniel Graupe, Co-advisor
Dan Schonfeld
Konstantin V Slavin, Neurosurgery
Leonard Verhagen-Metman, Rush University

ACKNOWLEDGMENTS

I would like to express my gratitude to Dr. Daniela Tuninetti and Dr. Daniel Graupe for giving me the opportunity to work with them. I am very grateful to them for their constant guidance and support, and am truly indebted to them for their patience and time.

I would like to sincerely thank Dr. Leonard Verhagen-Metman and Dr. Konstantin Slavin for their help with patient recruitment and data collection, for sharing their expertise in this vast field of movement disorders and for enabling this collaborative effort. I am very thankful to Jessica Karl, Dr. Ahmed Rabie and Feba Abraham for their assistance in data collection, and to all the patients who participated in this study. I would also like to express my appreciation for the contributions by Dr. Ishita Basu and Dr. Pitamber Shukla in this study.

I would like to thank Chirag Agarwal for the helpful and inspiring research discussions, to Jovita Rodrigues for being a wonderful roommate and to my friends for their help through my doctoral studies.

Last but not the least, I would like to thank my parents, Dr. Yadneshwar Khobragade and Dr. Sujata Khobragade, for their support, for being a constant source of encouragement and for the motivation when I needed it.

NK

TABLE OF CONTENTS

CHAPTER **PAGE**

1 INTRODUCTION 1
- 1.1 Deep Brain Stimulation 1
  - 1.1.1 Why close the loop? 2
- 1.2 Parkinson's Disease 3
  - 1.2.1 Etiology and Symptoms 3
  - 1.2.2 Pharmaceutical and Surgical interventions 3
- 1.3 Essential Tremor 4
  - 1.3.1 Etiology and Symptoms 4
  - 1.3.2 Pharmaceutical and Surgical interventions 5
- 1.4 Closed-loop DBS approaches: 5
  - 1.4.1 Neural activity based closed-loop DBS 7
  - 1.4.2 Peripheral sensors based closed-loop DBS 8
  - 1.4.3 Neurochemical control 9
  - 1.4.4 Volitional movement in ET 9
- 1.5 Past work 9
- 1.6 Goals and outline of this work 11

2 DATA COLLECTION AND MEASUREMENT OF DEGREE OF BENEFIT OF ON-DEMAND DBS 15
- 2.1 Data collection 15
- 2.2 Degree of Benefit 19
- 2.3 Optimal Duration of Stimulation 21
- 2.4 Who benefits from on-demand DBS system? 22

3 FEATURE EXTRACTION AND DESIGN OF TREMOR PREDICTION ALGORITHMS 25
- 3.1 Pre-processing and Feature Extraction 25
  - 3.1.1 Spectral measures 26
  - 3.1.2 Entropy measures 28
  - 3.1.3 Recurrence Quantification Analysis (RQA) 30
- 3.2 Machine Learning Algorithms 31
  - 3.2.1 Modified LAMSTAR Neural network 31
  - 3.2.2 Decision Tree Learning 35
  - 3.2.3 Minimax Support Vector Machine 36
- 3.3 Performance metrics 37

TABLE OF CONTENTS (Continued)

CHAPTER **PAGE**

4 COMPARISON OF PERFORMANCE OF TREMOR PREDICTION ALGORITHMS 41
4.1 Tremor prediction results 41
4.1.1 PD 43
4.1.2 ET 52
4.2 Discussion 56
4.2.1 Performance 56
4.2.2 Sensitivity 57
4.2.3 Accuracy 57
4.2.4 β-ratio 58

5 ON THE NEED FOR ADAPTIVE LEARNING IN ON-DEMAND DEEP BRAIN STIMULATION FOR MOVEMENT DISORDERS 59
5.1 Training and testing on data from different sessions 60
5.2 Comparison of performance 60
5.3 Need for adaptive learning 64

6 DETERMINATION OF DISTINCT PRE-TREMOR INTERVAL FROM SEMG DATA WITHIN TREMOR-FREE-STIMULATION-FREE PERIOD IN PD PATIENTS 67
6.1 Efficiency operator 68
6.2 Results 69
6.3 Conclusion 71

7 CONCLUSION AND FUTURE WORK 73
7.1 Conclusion 73
7.2 On-Demand closed-loop DBS in practice 74
7.2.1 Selecting Optimal duration of stimulation 75
7.2.2 Preventing Paresthesia 76
7.2.3 Rechargeables IPGs 76
7.2.4 Continuous learning 76
7.3 Future work 77
7.3.1 sEMG and acc signals recorded from free-moving patients 77
7.3.2 Extending to other disorders 77

APPENDICES 78

CITED LITERATURE 88
VITA 93

LIST OF TABLES

TABLE		PAGE
I	DETAILS OF PATIENTS AND DBS SETTING PARAMETERS	17
II	AVERAGE R_o AT DIFFERENT DS FOR PD1 - PD9	24
III	AVERAGE R_o AT DS^* FOR KINETIC, POSTURAL AND RESTING MODES	24
IV	PERFORMANCE OF DT AND LNN-2 IN TERMS OF ACCURACY AND SENSTIVITY FOR EIGHT PD PATIENTS	49
V	PERFORMANCE OF DT AND LNN-2 IN TERMS OF PREDICTED STIMULATION - FREE TIME FOR EIGHT PD PATIENTS	50
VI	PERFORMANCE OF DT AND LNN-2 IN TERMS OF PREDICTED STIMULATION - FREE TIME FOR EIGHT PD PATIENTS AT THEIR OPTIMAL DURATION OF STIMULATION	51
VII	PERFORMANCE OF DT AND LNN-2 IN TERMS OF ACCURACY AND SENSTIVITY FOR FOUR ET PATIENTS	54
VIII	PERFORMANCE OF DT AND LNN-2 IN TERMS OF PREDICTED STIMULATION - FREE TIME FOR FOUR ET PATIENTS	55
IX	PERFORMANCE METRICS: TRAINING AND TESTING ON DATA FROM THE SAME SESSION	62
X	PERFORMANCE METRICS: TRAINING AND TESTING ON DATA FROM DIFFERENT SESSIONS	63
XI	CHANGE IN ENTROPY AND MEAN FREQUENCY	70

LIST OF FIGURES

FIGURE		PAGE
1	On-demand DBS system schematic consisting of sensors (sEMG and Acc) on the tremor dominant limbs, a signal processor, machine learning algorithm and a wireless trigger relay.	6
2	Set-ups for acquisition of sEMG and accelerometer signals during Resting, Posture and Action states	17
3	Raw sEMG and acc signals: the data collection protocol with fixed duration of stimulation between 20-80 s	20
4	Architecture of LNN consisting of self-organizing maps and output layer connected by link weights that update based on Hebbian learning	32
5	Minimax hinge loss vs 0-1 loss and Hinge loss	37
6	Definitions of TP, TN, FP and FN for tremor prediction using machine learning algorithms	38
7	A "Rest" trial (stim duration = 30 s) with $True\ Positive$ prediction	44
8	Zoomed-in plot of sEMG and acc features for "Rest" trial with $True\ Positive$ prediction	45
9	An "Action" trial (stim duration = 50 s) with $True\ Positive$ prediction (separate modes) and $False\ Positive$ prediction (combined modes)	46
10	A "Posture" trial (stim duration = 30 s) with $True\ Negative$ prediction	47
11	Comparison between predicted and observed R-ratio when training and testing performed on the same session data	65
12	Comparison between predicted and observed R-ratio when training and testing performed on data from different sessions	65
13	delta N over 5 second windows of mean frequency	71

LIST OF ABBREVIATIONS

FDA	Food and Drug Administration
PD	Parkinson's Disease
ET	Essential Tremor
DBS	Deep Brain Stimulation
IPG	Implantable Pulse Generator
HFS	High Frequency Stimulation
BG	Basal Ganglia
VIM	Ventral Intermediate Nucleus
LFP	Local Field Potential
STN	Subthalamic Nucleus
GPi	Globus Pallidus interna
sEMG	surface-Electromyography
acc	Accelerometry
WT	Wavelet Transform
RQA	Recurrence Quantification Analysis
LAMSTAR	LArge Memory STorage And Retrieval
SOM	Self-Organizing Map

LIST OF ABBREVIATIONS (Continued)

WTA	Winner-Take-All
LNN-1	LAMSTAR Neural Network, type 1
LNN-2	LAMSTAR Neural Network, type 2 (normalized)
MDL	Minimum Description Length
DT	Decision Tree
CART	Classification And Regression Tree
BPNN	Back-Propagation Neural Network
DS	Duration of Stimulation
DS*	Duration of Stimulation (optimal)

SUMMARY

This thesis presents an automated tremor prediction algorithm based on modified Large memory storage and retrieval Neural Network (LNN-2), for the design of closed-loop Deep Brain Stimulation (DBS) system. The proposed method modifies the current open-loop paradigm of DBS to work on-demand by forecasting the onset of tremor in Parkinson's Disease (PD) and Essential Tremor (ET) patients. Feedback provided by non-invasive physiological signals is used to drive the DBS in an on-off regime, stimulating the target region only when required. Such closed-loop DBS systems, thereby reduce the amount of stimulation applied to the brain and may also lead to improving the battery life, decreasing the risk of infection due to repetitive battery replacement surgeries.

Previously, the proof-of-concept of such a closed-loop system was established using surface ElectroMyoGraphy (sEMG) and accelerometry (acc) signals in four PD and four ET patients. To detect the reappearance of tremor, thresholds were manually set on selected features. This process is tedious since the manual algorithm is patient-specific and the threshold parameters have to be chosen individually for each patient. To automate the process, Decision Tree (DT) algorithm was used and found to perform better than back-propagation neural network, and support vector machine methods. The Classification and Regression Tree (CART) algorithm used for DT will be compared here with LNN-2.

The main objectives of this thesis are:

1. Collect more data and assess the benefit of closed-loop DBS system in tremor-dominant PD patient population,

2. Automate the process of tremor prediction using LNN-2 approach and improve the accuracy and sensitivity of prediction,
3. Compare the algorithm with previously used DT method,
4. Assess the robustness of tremor predcition over time,
5. Determine a pre-tremor interval during the stimulation-free time using sEMG sensors.

Introduction to movement disorders, PD and ET, are given in the Chapter 1. Symptoms, cause and the therapeutic treatment methods for both the disorders are outlined followed by a brief description of DBS system in the current open-loop paradigm. Different feedback signals for closed-loop systems used in the past work are introduced here. Finally, the specific goals of this research work and its significance are stated.

Second chapter describes the process of patient recruitment and data collection. Two different set-ups have been used for recording the non-invasive sEMG and acc signals. This thesis introduces new data for four PD patients (second set-up). One more PD and two ET patients had participated in the study; however, were not good candidates for the closed-loop system. Their data has not been used for training or testing of prediction algorithms. In on-demand DBS systems, stimulation is only applied when the tremor is predicted to return after DBS is switched off. Data collected from nine PD patients showed that the duration of tremor-free stimulation-off time varied from patient to patient, with some patients having as little as 30 seconds to some patients having even more than three minutes of such tremor-free time. The benefit of closed-loop DBS system was quantified and assessed for these nine patients using metrics that give the ratio of stimulation-off time without tremor to the duration of stimulation. This was used to show who may benefit most from such on-demand systems and show the

importance of choosing the optimal duration of stimulation to maximize this ratio. To maximize the benefit and maximize the ratio of stimulation free time, an analysis of patient-specific optimal duration of stimulation is provided for PD patients. The tables list the observed ratio of stimulation-off, tremor-free time to the duration of stimulation for different durations of stimulation ranging 20-80 seconds.

Chapter 3 details the preprocessing and feature extraction, followed by a detailed description of the machine learning algorithms used. For the automation of tremor prediction, features were extracted from physiological signals recorded at the symptomatic extremities during Posture, Rest and Action states. Training and Testing was carried out using sEMG and acc based parameters, separately for each of the eight PD and four ET patients. LNN-2 is run for all the modes together (Action, Posture and Rest combined) and separately (Action state and Posture+Rest states). The architecture of LNN-1 and LNN-2 is included along with different methods of input discretization in place of self-organizing maps. LNN-2 is the modified version of LNN-1 with a minor change in the decision making process. In LNN-2, the link weights are normalized with respect to the number of times the winner neuron has fired. Comparison is made for these state-specific and states-combined methods and given in Chapter 4. Performance of state-specific run was better compared to the combined-states run. We also compare LNN-2 with Decision Tree (DT), using the same set of spectral, entropy and recurrence rate parameters for both the techniques as well as the same set of training and testing trials. DT algorithm, CART, which uses Gini index as split criterion, is then explained. For all the comparisons, the results are also given separately for trials at an optimal duration of stimulation that maximizes the ratio of stimulation free time without tremor to the duration of stimulation. In case of ET patients, results are given separately. LNN-2 was seen to perform better than DT algorithm.

SUMMARY (Continued)

In Chapter 5, the need for adaptive on-demand DBS systems is described. Data from two patients (PD and ET) who had two different sessions of recordings spaced by at least one week was used. Training and testing of the algorithms were then performed on the two different sessions. Tremor prediction performance metrics were then used to assess the robustness of on-demand DBS algorithms over time. The decline in performance between different sessions showed the need for adaptive learning of on-demand DBS systems.

Chapter 6 shows that a specific and distinct Pre-Tremor (PT) interval exists within the No-Stimulation-No-Tremor (NS-NT) period. This was shown using sample entropy and mean frequency features extracted from sEMG data in one tremor-dominant PD patient with high R-ratio. Identifying this PT interval when DBS is off in sEMG signal based features justify the use of sEMG sensors and are important to assess for on-demand predictive control of DBS.

Final chapter concludes this thesis on demand-driven DBS system based on machine learning approach applied to non-neuronal, peripheral sensors. The future work is also given in this chapter. Next, we would also like to conduct more sessions with patients in their natural state rather than in the controlled environment with fixed tasks that were used in the current protocol. Based on a bigger dataset, adaptive learning methods can be studied which could ensure robustness of closed-loop DBS systems over time. With the recent rise in wearable devices, we envisage a closed-loop system based on sEMG and acc signals for tremor-dominant PD and ET patients.

PUBLICATIONS AND AUTHOR CONTRIBUTIONS

Parts of the content of this thesis have been published in *Neuromodulation: Techonology at the Neural Interface*, *Proceedings of the 37nd Annual International Conference of the IEEE Engineering in Medicine and Biology Society*, *Proceedings of the 40th Annual International Conference of the IEEE Engineering in Medicine and Biology Society* and *European Journal of Translational Myology: Applied Myology*.

Chapter two deals with data collection and degree of benefit of on-demand DBS. The work was published in *Daniel Graupe, Nivedita Khobragade, Daniela Tuninetti, Ishita Basu, Konstantin Slavin, Leo Verhagen Metman: Who may benefit from on-demand control of DBS: a non-invasive Parkinson patients evaluation, Neuromodulation: Technology at the Neural Interface, 2018* for which I served as the second author. I was a major contributor to the paper where I collected data from five of nine patients. I computed the essential metrics for all patients leading to the key results that helped identify which patients would benefit from on-demand DBS and that an optimal duration of stimulation could help improve the efficacy of the system.

Parts of chapter 3 were presented in *Nivedita Khobragade, Daniel Graupe, Daniela Tuninetti: Towards fully automated closed-loop Deep Brain Stimulation in Parkinson's disease patients: A LAMSTAR-based tremor predictor, Engineering in Medicine and Biology Society (EMBC), 37th Annual International Conference of the IEEE, August 2015* for which I served as the first author. A different algorithm was applied to data collected from one PD patient.

PUBLICATIONS AND AUTHOR CONTRIBUTIONS (Continued)

Some parts of the thesis (Chapter 3 and Chapter 4) are to be submitted for publication as *Nivedita Khobragade, Daniela Tuninetti, Daniel Graupe, Leonard Verhagen, Konstantin Slavin, Ishita Basu: On-Demand Control of DBS Using Non-invasive EMG Sensors in Movement Disorders* where I will be the first author. The results were obtained from my work of feature extraction and implementation of machine learning algorithms for all patients. Parts of feature extraction are based on research from Dr. Ishita Basu.

Results in chapter 5 were presented in *Nivedita Khobragade, Daniela Tuninetti, Daniel Graupe: On the need for adaptive learning in on-demand Deep Brain Stimulation for Movement Disorders, Engineering in Medicine and Biology Society (EMBC), 40th Annual International Conference of the IEEE, July 2018* where I served as the first author and obtained the presented results.

Parts of chapter 6 are to be submitted for publication as *Daniel Graupe, Nivedita Khobragade, Konstantin Slavin, Leo Verhagen Metman, Daniela Tuninetti, Ishita Basu : Determining Unique Pre-tremor Phase within Tremor-free-Stimulation-free Period in sEMG Data of DBS-Implanted PD Patients*. I served as the second author and performed data collection and helped with parts of the analysis.

Parts of the Chapter 7 are to be submitted for publication as *Nivedita Khobragade, Daniela Tuninetti, Daniel Graupe, Leonard Verhagen, Konstantin Slavin, Ishita Basu: On-Demand Control of DBS Using Non-invasive EMG Sensors in Movement Disorders* where I will be the first author. This chapter deals with conclusion and considerations to be made for using on-demand DBS system in practice.

CHAPTER 1

INTRODUCTION

1.1 Deep Brain Stimulation

Deep Brain Stimulation (DBS) is a therapeutic surgical procedure that was approved by the FDA in 1997 for parkinsonian and essential tremor (ET). DBS originated from the work by Benabid *et al* [1], who first applied it to Parkinson's Disease (PD) and has since been extended for the treatment of a range of other neuromotor and neuropsychiatric disorders. The device controls the symptoms by applying continuous High-Frequency Stimulation (HFS) to the intended target regions in the brain. This well-established implant is estimated to have been received by more than 100,000 patients worldwide [2, 3]. DBS does not cure the disorder but helps with its management resulting in an overall improvement of quality of life. Unlike the lesioning surgical interventions such as thalamotomy for PD and ET, DBS is reversible and adjustable allowing original state to be restored.

A typical DBS system consists of a macroelectrode, an Implantable Pulse Generator (IPG) and an extension wire connecting the two. The macroelectrode or the lead is implanted at the target location which is selected based on the disorder and the related symptoms. The IPG, implanted subcutaneously below the clavicle, is used to send the pulses to the lead and to control the HFS parameters. Once the parameters are set, the stimulation is applied continuously to the target regions. DBS systems have evolved in the past two decades in terms of the macroelectrode design, the stimulation paradigms, and ongoing research towards adaptive stimulation systems. Although DBS technology has advanced, com-

mercially available systems still run in open-loop mode, where HFS of fixed amplitude, frequency and pulse width is delivered continuously without adapting to the symptoms.

1.1.1 Why close the loop?

Although this treatment is widely accepted, the mechanism of DBS is not yet completely understood. The present-day DBS systems available in the market work open loop which means that the stimulation is applied continuously without identifying the onset of symptoms. DBS, though reversible, can lead to some unwanted side-effects such as dysarthria, gait impairment and dyskinesia [4]. These side-effects may be mitigated using interleaving and field shaping techniques by reducing the stimulation of undesirable regions. Interleaving approach uses varying stimulation parameters on different sets of contacts, thereby stimulating different areas in alternating fashion and alleviating stimulation-induced side-effects. However, this approach can increase the battery drain [5]. Field shaping by selection of the optimal contact segments may also help reduce such side-effects [6]; albeit still applying stimulation continuously when run open-loop. An effective system would minimize these undesirable effects while maximizing the therapeutic effect of the stimulation. It has been previously shown that adaptive and on-demand closed-loop DBS systems provide more effective symptom management with reduced side-effects and improved power saving [7, 8].

An on-demand system can achieve improved efficacy can be achieved by applying stimulation only when required. Such a system would, as a result, also increase the battery life of the device. The battery of the IPG delivering HFS, needs to be surgically replaced every 3 to 4 years. Incidence of infection has been reported to increase with number of IPG replacements [9]. By improving the battery life, such traumatic surgeries, the associated risk of postoperative infection and the cumulative costs can

be reduced. An on-demand system can be designed to track a suitable feedback signal specific to the disorder and apply stimulation only when necessary. For movement disorders such as PD and ET, DBS can be applied in a closed-loop regime by monitoring and predicting the onset of tremor.

1.2 Parkinson's Disease

1.2.1 Etiology and Symptoms

PD is a progressive neurological movement disorder, characterized mainly by motor symptoms such as tremor, bradykinesia, rigidity, and axial symptoms related to gait and balance issues. It is one of the most prevalent neurodegenerative diseases, second only to Alzheimer's disease [10]. It is caused by degeneration of dopamine-producing cells in the substantia nigra, a component of the Basal Ganglia (BG) motor pathway in the brain. PD phenotypes are classified as Tremor-Dominant (TD) and Non-Tremor Dominant (NTD) which includes postural instability and gait disability (PIGD) subtype and PD subtype dominated by bradykinesia and rigidity [11]. Resting tremor is the most common symptom seen in PD patients. These patients may also experience kinetic tremors while performing voluntary movement. Tremors are observed to be prominent towards the distal ends of the limbs [12]. The frequency of resting tremors lie in 4-6 Hz and the postural or kinetic tremors are in the range of 7-11 Hz [13].

1.2.2 Pharmaceutical and Surgical interventions

In early stages of PD, the symptoms can be controlled by pharmacological treatment of Levodopa-Carbidopa, albeit not permanent. As the disease progresses, this drug combination is no longer adequate to curb the debilitating symptoms. At this advanced stage, the patients are recommended the surgical intervention of DBS.

In case of PD patients, the DBS macroelectrode is stereotactically implanted in one of the two target sites, either Sub-Thalamic Nucleus (STN) or Globus Pallidus interna (GPi). This electrode is connected to an IPG or the neurostimulator, which is surgically placed below the clavicle. Each macroelectrode consists of four contacts of which two are selected. Different combinations of contacts give different field distributions, thereby stimulating different extents of the target region. IPG can be programmed externally by the clinician by evaluating the effect of each configuration on the symptoms. The combination of contacts and the parameters of the HFS, such as amplitude, frequency, pulse width, are set to maximize efficacy and minimize any side-effects. IPG then provides HFS of the set parameters continuously to the target location.

Frequently, DBS leads to certain side-effects such as dysarthria and gait impairment in PD patients. STN-DBS may lead to dysarthria which means patients may experience speech impairment including speech slurring and intelligibility [14]. Though DBS improves PD symptoms as well as levodopa-induced dyskinesia, in some cases stimulation of upper portion of STN may even exacerbate dyskinesia [15]. Such Stimulation-Induced Dyskinesia (SID) was observed to most commonly be manifested in the contralateral lower limb. Such side-effects reduce the efficacy of DBS systems. It is, therefore, imperative to reduce these side-effects while still providing the benefits of the conventional open-loop DBS. Adaptive and on-demand DBS systems can help curb such side-effects [16].

1.3 Essential Tremor

1.3.1 Etiology and Symptoms

ET is another prevalent movement disorder, and is characterized by tremor in 4-12 Hz range [17]. Unlike PD, tremor in ET patients appear only when effort is exerted. These rhythmic oscillations occur

during voluntary movement with higher amplitude of kinetic tremor than that of postural tremor. The amplitude also increases during intentional tasks when the target is approached. The pathophysiology of ET is unknown and it cannot be cured.

1.3.2 Pharmaceutical and Surgical interventions

The symptoms of ET can be controlled by drug intervention of propranolol and primidone. As the disease advances, surgical options are considered. Lesioning method of thalamotomy is irreversible where a permanent lesion to thalamus is applied. DBS is another surgical option which is an invasive approach but is reversible. The electrode is placed in Ventral Intermediate Nucleus (VIM) of thalamus and continuous HFS is applied to disrupt the pathological oscillations in the thalamocortical circuit [18].

VIM stimulation side-effects include speech slurring, increased falls and drooping of eyes. The currently available DBS systems run open-loop, and the IPG runs continuously irrespective of whether stimulation is required or not; however, since the kinetic tremors in ET are initiated by volitional movement, the amount of stimulation to the target brain region and the side-effects can be reduced by enabling DBS only when the patient is using their affected limb [19,20]. This may potentially improve the battery life as well.

1.4 Closed-loop DBS approaches:

Closed-loop DBS system receives feedback from a signal that enables the stimulation to adapt with the disease symptoms [21]. The adaptive control methodology for closed-loop DBS can be divided into two classes: i) On-demand binary approach where the stimulation is either on or off based on presence or absence of symptoms and ii) scalar approach where the stimulation voltage is modulated by monitoring biomarkers [8]. Both the approaches can be implemented using either implanted or

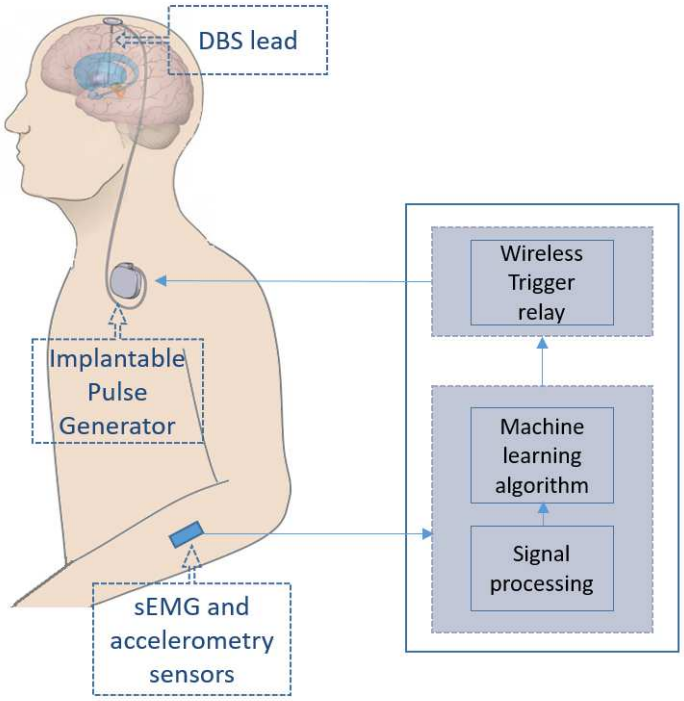

Figure 1. On-demand DBS system schematic consisting of sensors (sEMG and Acc) on the tremor dominant limbs, a signal processor, machine learning algorithm and a wireless trigger relay.

noninvasive sensors. These adaptive systems modulate the stimulation by using a control sigal with information indicative of the symptoms. For prediction of onset of tremor, a variety of approaches can be adopted which are described in the following sections. Signals such as Local Field Potential (LFP), surface Electromyography (sEMG), Electroencephalography (EEG) and kinematic signal from gyroscope have been employed for tracking or predicting tremor onset [16, 20, 22, 23].

1.4.1 Neural activity based closed-loop DBS

The neural signals such as LFP or Single Unit Spike (SUS) can provide information regarding symptom reoccurence. These signals can be recorded from a separate microelectrode placed close to the target region of stimulation or from a bidirectional recording and stimulating macroelectrode.

1.4.1.1 SUS as feedback signal

In [7], Rosin *et al* showed a superior control of Parkinsonian symptoms in 1-methyl-4-phenyl-1, 2, 3, 6-tetrahydropyridine (MPTP)-treated primate model using closed-loop DBS system than by open-loop continuous stimulation despite less overall stimulation. Action potentials in the primary motor cortex were monitored and stimulation was applied to GPi on occurrence of a spike in M1, coinciding with the BG-cortical loop oscillations. Since chronic recording of a single M1 spike may not be reliable, this procedure is not conducive for long-term implementation [24]. Following the success of closed-loop DBS in a non-human primate model, different strategies have been applied for extending this closed-loop approach to human subjects using more reliable signals such as Local Field Potentials (LFP).

1.4.1.2 LFP biomarkers

Neuronal signals can be measured as feedback from the site of stimulation for prediction of tremor and other Parkinsonian traits. An elevated beta band power associated with bradykinesia and rigidity has been observed in the LFPs recorded from STN. A simple approach of tracking LFP beta power was shown by [16] and [25]. The stimulation would be triggered once the beta power crossed a certain threshold, controlling DBS in a binary on-off fashion in [16]. A scalar adaptive DBS (aDBS) in a freely moving patient were tested by Rosa *et al*. The stimulation amplitude is modulated to adapt to the LFP

beta power changes. These methods using LFP as a biomarker require changes to the DBS electrode to either perform both stimulation and recording or need an additional electrode at the site dedicated for measurement of neural activity and communicating with the IPG.

1.4.2 Peripheral sensors based closed-loop DBS

The increase of beta power in LFPs is associated with bradykinesia and rigidity, but not tremor, which is a cardinal sign of PD. This increase is absent in one-third of the patients [21]. It can, therefore, not be invariably used as the indicative biomarker [6]. A different indicator is required for on-demand DBS control for tremor-dominant disorders, such as those of interest in this work. Of all the symptoms, tremor is the first one of the PD clinical signs to reappear on switching off the stimulation [26]. Prediction of this symptom can, thus, be used as an indication for switching on the stimulation in a demand-driven system. Peripheral wearable devices such as sEMG sensors, and gyroscopes have been used to track tremor for closed-loop DBS [21].

1.4.2.1 Electromyography and accelerometry signals

Non-neuronal signals recorded from peripheral sensors, such as, surface Electromyography (sEMG) and accelerometer (acc), can also be used to extract predictive information regarding tremor. Proof-of-concept of an on-demand DBS system using sEMG and acc signals was presented in [22]. Both these sensors are non-invasive. The newer generations of this additional hardware are comfortable, smaller in size and no longer bulky. With the recent rise in the use of wearable devices, there is a reduced stigma towards wearing such monitoring devices [27]. Tremor prediction could also just be an additional functionality of an activity-tracking wearable device.

1.4.2.2 Inertial measurement unit signals

Similar to using these wearable sensors , a kinematic aDBS for resting tremor was described in [23]. Tremor power in 4-8 Hz was estimated by employing a gyroscope to adaptively modulate the stimulation voltage. Stimulation was switched off when the tremor power was below 25% of its maximum value.

A combination of neural and wearable signals can be used to predict tremor and non-tremor symptoms together.

1.4.3 Neurochemical control

In [28], a closed-loop DBS system based on monitoring neurochemical changes is proposed. The dopamine level changes were used to set the stimulation in rodent PD model. Irrespective of the biomarker used for designing closed-loop DBS, all the strategies are suggested to lead to physiological improvement and reduction in battery consumption [29].

1.4.4 Volitional movement in ET

Such demand-driven control for DBS systems can similarly be employed for other motor disorders. Since tremor appears only during voluntary movement in essential tremor, an on-demand DBS system can be implemented for this neuromotor disorder by detecting movement intention alone. This can be identified by the decrease in low frequency beta oscillations using Electrocorticography [30] or recognizing intent of motion using EMG signals [31].

1.5 Past work

An on-demand DBS system should maximize accurate tremor prediction so that the patient does not suffer any discomfort. It should also minimize early predictions or false alarms due to voluntary movement being erroneously interpreted as tremor. By implementing such a closed-loop system, it may

be possible to increase the battery life of the IPG and also mitigate the adverse effects of continuous stimulation. In [22], a non-invasive DBS system was presented which would run on-demand as an add-on system to the current DBS set-up without any modifications to the stimulating electrodes or the IPG. A stimulation of fixed duration is to be applied and once stimulation is turned off, an algorithm would track certain parameters obtained by processing sEMG and acc signals. The onset of tremor is predicted using a set of thresholds applied to these features. Once the tremor is predicted, the stimulation would be switched on again. The thresholds were set manually for each of the four PD patients and an accuracy of 80.2% with 100% sensitivity was achieved. Since PD is progressive and rapidly changing, this process may not be conducive for a larger number of patients. To automate this process, a Back-Propagation Neural Network (BPNN) was applied in [32, 33]. An overall accuracy of 76% and sensitivity of 92% was obtained for four patients, with sensitivity ranging from 88.9% to 93.3%. Sensitivity of 100% is required to ensure that the patient does not experience tremor during stimulation off period.

LArge Memory STorage And Retrieval (LAMSTAR) neural network was applied to one patient in [34]. The performance of LAMSTAR neural network (LNN-1) for one patient was found to be better than BPNN, with 77% accuracy and 100% sensitivity. LAMSTAR is based on the concepts of winner-take-all (WTA) and Hebbian learning. It consists of multiple Self-Organizing Map (SOM) layers which take different features as inputs. Each SOM layer contains neurons of which only one "winner" neuron fires for the given input. By Hebbian learning, the synaptic weights connecting each SOM neuron to the decision layer neurons are increased when that neuron fires for the given output decision neuron. The more probable output is determined by comparing the sum of link weights from the winner SOM neurons to each of the output layer neurons. In [34], LNN-1 was used where link weights are not

normalized. We denote the modified network with normalized link weights as LNN-2, described in the next section.

1.6 Goals and outline of this work

In past work [33], Decision Tree (DT) was found to perform better than machine learning algorithms such as BPNN, for prediction of tremor in four PD patients. These set of algorithms were used in offline learning mode where training and testing are done separately and the thresholds (as in DT) or weights (as in BPNN) once set, remain unchanged, irrespective of the changes in the characteristics of the disorder. The goals for designing an effective closed-loop DBS system are:

1. To design an automated tremor prediction algorithm based on non-invasive physiological signals. LNN-1 has been used previously for medical diagnosis and prediction applications such as automated detection of epileptic seizures using features extracted from electroencephalography signals [35] and apnea episodes prediction using submental EMG-based features [36]. If such networks are run in online learning mode, updating link weights with each new instance of data, they can adapt with the changes in symptoms. Use of such algorithms in the design of closed-loop system helps adjust thresholds with progression of the disease. Offline learning methods need to be trained at regular intervals and do not adapt with the changes in disease features. Due to limited duration of data for each patient, we have used offline learning methods for training.

2. To improve the performance of the algorithm so as to increase accuracy by reducing the number of false alarms as well as to obtain 100% sensitivity and make sure that false negatives are minimum. LNN-1 can be improved by normalizing these link weights by the number of times the

winner neuron of SOM layer fires with respect to the corresponding output [37, 38] in LNN-2. Performance of LNN-2 is also compared with DT in offline learning mode for fair comparison.

3. To analyse the importance of selection of optimal duration of stimulation to maximize the benefit of a closed-loop DBS system. Ratio of stimulation-free time without tremor to the duration of stimulation was compared for different durations of stimulation.
4. To assess the robustness of on-demand systems over chronic use. Though the accuracy of the algorithms is improved, it is essential to check if the algorithms are able to perform well over time.
5. To detect changes in features that may be indicative of pre-tremor duration and can potentially be used for design of adaptive systems.

In this thesis, an on-demand DBS system is presented which is designed using LNN-2 for tremor prediction in eight PD and four ET patients. LNN-2 set-up is explained in detail in the next chapter. The performance and ratio of predicted stimulation-free time without tremor to the duration of stimulation of LNN-2 run for different limb states combined are compared with LNN-2 run for Action and Posture/ Rest states separately for 163 trials. The results are also presented for optimal durations of stimulation for each patient. Higher stimulation-free time percentages were obtained for the 59 trials at optimal duration of stimulation in eight PD patients.

The next set of comparisons were carried out for tremor prediction using LNN-2 and DT in offline mode for the same eight PD patients and four ET patients. In DT learning, a binary tree is generated for the given data. Gini impurity is used to decide the feature and the best split at each node. By using the split as a threshold on the selected feature, the data is divided into smaller subsets. Working top-

down, best features and splits are found for these small subsets and the process is repeated till the Gini impurity is zero which is obtained when the data at that node belong to same category. LNN-2 and DT are advantageous over BPNN since the training is faster compared to BPNN, which uses the gradient-descent algorithm and delta-rule for weight updates. They perform well with large datasets and can handle features of different data types. LNN-2 has other advantages such as the fast retrieval feature, the forgetting feature and correlation layer for related attributes, extensively discussed in [38]. Both the methods have properties of transparency and easy interpretability. For LNN, training can be continued during the "testing" phase without any added complexity. Once the initial weights are established, online learning with each new input-word continues during the operational run, allowing the network to keep adapting [38]. For closed-loop DBS, LNN can be enabled to continuously train with new data in a supervised manner by updating weights until the trigger event, tremor, appears. Iterative induction of DT can allow online learning of this algorithm as well which will be compared with LNN in future work. The two algorithms also have certain limitations. DT works in a greedy manner, finding the local optimal solution at each node. It may create a complex overfitted tree which can be overcome by pruning the tree to make it generalize better for new data. The classic LAMSTAR setup uses SOM modules which set the ranges in an unsupervised manner for each feature. For small dataset where clusters are not well-defined, unsupervised setting of thresholds may lead to not obtaining the required set of thresholds or using more neurons than required. This can be fixed by using a supervised binning method followed by the WTA principle. LNN-2 performed better that DT for both PD and ET patients.

The training of these machine learning algorithms has to be done separately for each patient since the symptoms and the signal features may be patient specific. A state-classifier needs to be designed

to accurately classify between Action and Posture / Rest states before the feature set is input to the corresponding tremor-predictor. We also intend to carry out data collection in free-moving patients to analyse the feasibility of wearable-based closed-loop DBS systems. The system can be used as an add-on system to the market-available open-loop DBS systems including the kind with rechargeable IPG batteries. The non-invasive wearable with sEMG and acc sensors can send trigger signals on prediction of onset of tremor to the telemetry module of the IPG and start the fixed optimal duration of stimulation. Tremor-predictor algorithm can adapt to the disease progression by learning online with each new instance of data. The conclusions and future work is discussed in the last chapter.

CHAPTER 2

DATA COLLECTION AND MEASUREMENT OF DEGREE OF BENEFIT OF ON-DEMAND DBS

Some sections of this chapter were published in Daniel Graupe, Nivedita Khobragade, Daniela Tuninetti, Ishita Basu, Konstantin Slavin, Leo Verhagen Metman: Who may benefit from on-demand control of DBS: a non-invasive Parkinson patients evaluation, Neuromodulation: Technology at the Neural Interface, 2018.

On-demand control of DBS in PD is based on the observation that interruption of stimulation is followed by a finite period that is free of PD symptoms with tremor being the first symptom to reemerge [26]. Such a system can be realized via non-invasive add-on surface EMG sensors placed on the patient's limbs to predict tremor. These sensors would communicate the "stimulation on" trigger to the IPG through an external device as in Medtronic Activa PC + S and Nexus-D interfacing system. In the following two sections, the procedures for patient recruitment and data collection are described along with test process for determination of degree of benefit of on-demand DBS system to individual PD patients.

2.1 Data collection

Nine patients with tremor-dominant PD and six patients with ET were recruited from the Movement Disorder Clinic at Rush University Medical Center in Chicago. The data collection was carried out at

University of Illinois at Chicago, Neuroscience Center under the UIC-IRB 2008-0971. Inclusion criteria for recruiting patients in this study were:

- patient is affected by TDPD or ET with tremor in one or more limbs ,
- patient has FDA-approved Medtronic DBS systems implanted in the STN or VIM at least 3 months before (details in Table 2.1),
- symptoms are well-controlled by medication and stimulation.

The patients were made aware of HIPAA compliance and informed consent was obtained before recording the data. All patients were on their usual medication during the recording session. One of the nine PD patients (PD6) was called for a second session since he had prolonged tremor-free period after withdrawal of stimulation and made for a good candidate for this study. One of the six ET patients (ET1) also had two separate sessions. In all, ten PD datasets (163 trials) and seven ET datasets (144 trials) were collected from nine PD and six ET patients. One patient (PD9) and two ET (ET5 and ET6) were excluded since the patients did not have well-controlled tremor which reappeared as soon as the stimulation was switched off.

To extract tremor predictive information non-invasively, sEMG and acc signals were measured from the tremor-dominant limbs of nine PD and six ET patients. Two different set-ups were used for the data collection with the only difference being in the sensors used. Figure 2.1 shows both the set-ups used for data collection. Placement of sEMG sensors on Extensor and Flexor muscles and a separate accelerometer sensor placed on the dorsal side of the tremor-dominant hand for the first set-up are shown in (a) and (c). The second set-up where wireless sEMG sensors with in-built accelerometers were placed on the Extensor and Flexor muscles are shown in (b), (d), (e) and (f).

TABLE I

DETAILS OF PATIENTS AND DBS SETTING PARAMETERS

Patient	Age	Gender	Implanted in (Year)	Amplitude	Frequency (Hz)	Pulse width (μs)	Contacts	Hand tested
PD1	46	M	2008	2.8 V	180	80	1-0+	Right
PD2	45	M	2002	2.5 V	185	60	1-2-C+	Left
PD3	52	F	2004	2.8 V	185	120	0-C+	Right
PD4	60	F	2009	2 V	145	60	1-3-C+	Right
PD5	60	F	2009	2.6 mA	125	450	1-3+	Right
				2.6 mA	125	90	3-0+	Right
PD6	69	M	2011	3.9 V	130	80	1-C+	Right
PD7	67	F	2001	3.5 V	185	120	1+2-C+	Right
PD8	62	M	2012	3.1 V	160	80	1-2-C+	Right
ET1	64	M	2002	2 V	150	90	2-C+	Right
ET2	67	M	2010	1 V	130	120	1-C+	Right
				1.4 V			5-6-C+	Left
ET3	51	M	2010	2.3 V	185	60	9-C+	Right
ET4	62	F	2007	2 V	185	90	0-C+	Right

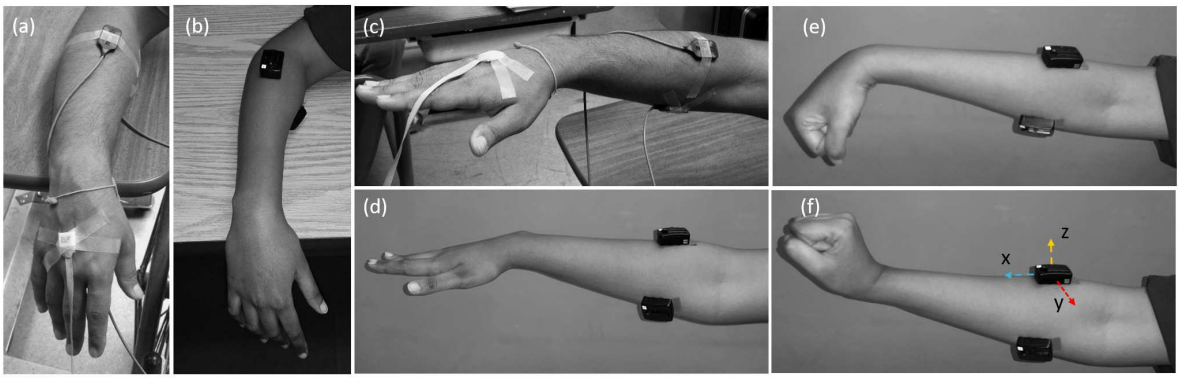

Figure 2. Set-ups for acquisition of sEMG and accelerometer signals during Resting, Posture and Action states

In the first set-up for eight patients (PD1 to PD4, ET1 to ET4), a Coulbourn type V94-41 miniature solid-state piezoresistive accelerometer sensor was placed 2 cm proximal to the middle metacarpophalangeal joint. sEMG was recorded in the first set-up using Delsys Bagnoli system. sEMG was recorded from the extensor digitorum communis and flexor digitorum profundus (forearm extensor and flexor muscles respectively) of the patient. Since tremor frequencies are different during relaxed states and during active states, multiple trials were carried out in three different states of Resting, Posture and Action. Figure 2.1 (a) shows Resting state where the arm is relaxed and is placed on a support. Posture state is shown in Figure 2.1 (c). Here, the arm is extended and held in a steady position.

In the second set-up for seven patients (PD5, PD6_1, PD6_2, PD7, PD8, PD9, ET5, and ET6), Delsys Trigno wireless sensors were used for measuring muscle activity. These devices also consist of in-built tri-axial accelerometer sensors; therefore, no additional accelerometer sensor was used. The wireless sEMG sensors minimize any motion artifacts. Figures 2.1 (b) and 2.1 (d) show Resting and Posture states, respectively. Figures 2.1 (e) and 2.1 (f) show the Action state where wrist extension and flexion was carried out continuously. Baseline recording was also done to ensure correct placement of the sensors. Sampling rate of sEMG and acc sensors in the first set-up was 1000 Hz where as in second set-up, the sEMG and acc signals were sampled at 1926 Hz and 148 Hz, respectively. Both the Delsys sEMG sensors, Bagnoli and Trigno, have in-built band-pass filtering 20 Hz and 450 Hz to reject movement artifacts as well as high-frequency noise. The tremor information, which lies in 5-12 Hz, can be recovered by envelope detection [22].

Patient was seated on a chair in an upright position with arms resting on a supporting surface as in Figures 2.1 (a) and 2.1 (b). Programmer interface which controls IPG, was placed on the IPG to

switch the DBS on or off. DBS was switched off at the beginning of the trial, followed by stimulation for a fixed duration. Stimulation remained in "off" state till tremor reappeared. sEMG and acc signals were recorded for the whole trial. Multiple trials were carried out for different durations of stimulation (DS: 20, 30, .. upto 80 seconds) and different states of resting, posture and action. In posture state, the patients arms were held out in an extended position with no support (Figures 2.1 (c) and 2.1 (d)). This posture was maintained without much movement. In the action state, the patient was asked to perform a task such as extending and flexing the wrist or reaching for the opposite shoulder (Figures 2.1 (e) and 2.1 (f)). Timestamps were noted for the events when stimulation was stopped, voluntary movement was started (action or posture) and tremor was observed after the stimulation was switched off.

Raw signals measured from the extensor muscle for Action trial are shown in Figure 3: sEMG (top) and y-axis signal of tri-axial accelerometer (bottom). Dashed black line indicates the time where stimulation was switched off. Vertical dashed green line shows the time of start of voluntary movement and red vertical line indicates the time of observed onset of tremor.

2.2 Degree of Benefit

During the recordings conducted over multiple patients, it was observed that the duration of time before tremor returned varied from patient to patient with some having the tremor return in less than 20 seconds after DBS was switched off and some having tremor not return for even more than three minutes. This showed that an on-demand DBS system may be more beneficial for some patients compared to others, given the predictions are made accurately as well as not too early compared to the actual observed tremor. Considering that the maximum benefit would be achieved with perfect prediction, the effectiveness of on-demand on-off DBS control for individual patients was quantified by calculating

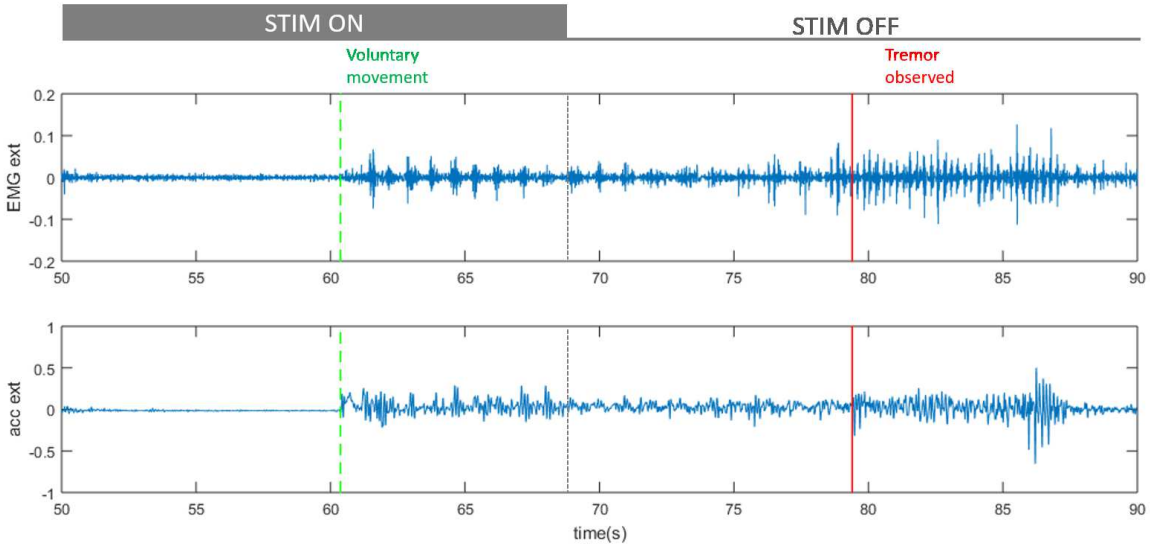

Figure 3. Raw sEMG and acc signals: the data collection protocol with fixed duration of stimulation between 20-80 s

the ratio of stimulation-off duration without tremor to the stimulation-on period. Higher ratio indicates greater benefit for such patients. Parameter R_o is defined as the observed ratio of stimulation-free time without tremor to the DS given by:

$$R_o = \frac{(T_{trem} - T_o)}{(T_o - T_s)} = \frac{(T_{trem} - T_o)}{DS} \tag{2.1}$$

where T_s denotes time of start of stimulation, T_{trem} is the time of reappearance of tremor before restarting stimulation, T_o is the time of end of stimulation, and DS = (T_o - T_s). R_o metric was calculated for all testing cycles during resting, postural, and kinetic states. Stimulation of different durations were

applied and the time of return of tremor was noted. It was observed that tremor may return in around the amount of same time or less even if the DS was higher indicating that longer DS may not be required and should be selected so as to maximize the R_o value.

Another metric to quantify the R_o information is the percentage of stimulation-free time which is more intuitive to understand given their values. The R_o values lead to the derivation of the percentage of stimulation-free time of the total time which is given by:

$$P_{sf}(\%) = \frac{R_o}{(1+R_o)}.100 = \frac{(T_{trem} - T_o)}{(T_{trem} - T_s)}.100 \tag{2.2}$$

For an average R_o of 1, the percentage $P_{sf}(\%)$ is 50% of total time, while R_o yields $P_{sf}(\%)$ of 80%. The trials described in the previous section consisted of DS in increments of 10 seconds for which the average of R_o ratio is given in Table II.

2.3 Optimal Duration of Stimulation

For an on-demand DBS system, larger is the R_o, the higher is the P_{sf} (%) and the better may be the patients benefit. It is, therefore, essential to find the optimal DS^* which maximizes this ratio, R_o, thereby maximizing the P_{sf} (%). Table II lists the R_o values for DS durations of 20-80 seconds with the maximum value given in bold for all the movement modes combined. The DS corresponding to the maximum R_o is the optimal duration of stimulation for the patient. For patients PD1, PD4, PD6, and PD8, tremor did not reappear till the end of cycle for some trials. The cycle was ended due to time restriction and time at the end of trial was used for calculation of Ro. This metric may, therefore, have been higher than the value given in the table and is indicated by a + symbol.

The optimal duration of stimulation (DS^*) can be selected based on the highest ratio on average for a given DS and is given along with P_{sf} (%) at DS^* in Table III. Average R_o at DS^* are given individually for the kinetic, postural and resting states with their corresponding number of tests. The same trend of higher R_o using optimal DS^* was observed in all patients during different states of resting, postural, and kinetic action of the tremor-dominant limb. Tests on one of the patients (PD3) were carried out at DS of 40 and 50 sec and were inadequate for this study. As a result, best DS^* was not examined for patient PD3. Therefore, the results for PD3 could not serve for comparison when analyzing the results that involve performance at optimal DS^*.

2.4 Who benefits from on-demand DBS system?

$P_{sf}(\%)$ gives the maximum possible percentage of time which would be stimulation-free with no tremor. In three of these eight patients, the average Ro is greater than 1, namely, 1.069 for PD4, 4.239 for PD6, and 2.07 for PD8, which means $>$50% stimulation free time at these optimal DS^*, while all the rest have an average Ro from 0.554 to 0.836 which on average gives 35% stimulation free time. We note that certain tests of PD1, PD4, PD6, and PD8 had to be terminated for lack of time before tremor could be observed. Therefore, in these tests, the average values of R_o might have been higher than is tabulated. In individual trials counted toward the tabulated averages, Ro was as high as 9.9 (case of PD6), and even this test was interrupted before any tremor was observed due to time limitations).

The results in Table III indicates that there exists a subset of PD patients that may benefit rather significantly from on-demand control. Using metrics, R_o and $P_{sf}(\%)$, the possible benefit of on-demand DBS system can be evaluated; however, in practice, the $P_{sf}(\%)$ depends on the performance of the

predictive algorithm. A similar metric as R_o can be used to evaluate the average stimulation-free time when using an on-demand system. This can be given as:

$$R_p = \frac{(T_{pr} - T_o)}{DS} \tag{2.3}$$

where T_{pr} is the predicted time of reappearance of tremor before restarting stimulation, T_o is the time of end of stimulation, and DS is the duration of stimulation.

By maximizing the stimulation-free time without tremor by making accurate prediction of tremor, the side-effects such as speech dysarthria may potentially be reduced. Based on the DS^* and R_o values, the benefit of on-demand DBS for a patient given their side-effects to DBS can be evaluated by the clinician. More patients need to be tested to decide if the observation of symptoms other than tremor would help in selection of DS^* in patients with non tremor-dominant PD.

TABLE II. AVERAGE R_o AT DIFFERENT DS FOR PD1 - PD9

Patients	Average R_o at DS (sec)						# of tests	
	20	30	40	50	60	80	at all DS	with no tremor
PD1	-	**0.68+**	0.39	-	-	-	16	2
PD2	**0.84**	0.63	0.52	0.43	-	-	26	0
PD3	-	-	0.3	0.15	-	-	17	0
PD4	**1.069+**	0.87	0.76	0.59			32	2
PD5	-	**0.554**	0.3	0.1	0.21	0.145	20	0
PD6	-	**4.24+**	-	0.96	-	-	29	12
PD7	-	**0.73**	-	0.16	-	0.22	9	0
PD8	-	**2.07+**	1.29	0.234		-	14	2
PD9	-	0.585	-	0.14		-	4	0
Total							167	18

TABLE III. AVERAGE R_o AT DS^* FOR KINETIC, POSTURAL AND RESTING MODES

Patients	Average R_o at DS^* (sec)						$P_{sf}(\%)$ at DS^*
	Kinetic	# of tests	Postural	# of tests	Resting	# of tests	
PD1	0.96	3	0.31	3	0.84	2	40.48
PD2	1.09	1	0.80	3	0.76	2	45.36
PD3	-	-	-	-	-	-	
PD4	0.46	2	1.32	3	1.23	3	51.69
PD5	-	-	0.69	1	0.42	1	35.48
PD6	2.81	11	5.43	7	5.46	6	80.88
PD7	1.48	1	0.50	1	0.18	1	44.13
PD8	0.44	4	1.83	4	8.14	1	67.43
PD9	0.80	1	-	-	0.37	1	36.95
Total		23		22		17	

CHAPTER 3

FEATURE EXTRACTION AND DESIGN OF TREMOR PREDICTION ALGORITHMS

Some sections of this chapter were published in Nivedita Khobragade, Daniel Graupe, Daniela Tuninetti: Towards fully automated closed-loop Deep Brain Stimulation in Parkinson's disease patients: A LAMSTAR-based tremor predictor, Engineering in Medicine and Biology Society (EMBC), 37th Annual International Conference of the IEEE, August 2015 ©and some sections are to be submitted for publication.

In this chapter, feature engineering from the sEMG signals to extract information related to onset of tremor and the setups of different machine learning algorithms for the design of an on-demand DBS system, are described.

3.1 Pre-processing and Feature Extraction

Attributes for the machine learning algorithms were extracted by performing spectral, entropy and recurrence quantification analysis on extensor and flexor sEMG. Spectral analysis was also carried out on acc signal. In case of the first set-up, accelerometer sensor measured the magnitude of the signal recorded from the location shown in Figure 2.1 (a). For the second set-up, each of the sensors placed on extensor and flexor, recorded accelerometer along the three axes. We found that for these locations, it was more useful to consider each axis information separately than the magnitude.

The raw sEMG signals were smoothened first, by calculating the power over a window of 50 ms at every sample. Spectral, entropy and recurrence parameters were then calculated over sliding windows of 1 second with an overlap of 750 ms of the smoothened sEMG and acc signals as in [22]. Following is a description of the features used for tremor prediction:

3.1.1 Spectral measures

Tremor information typically lies in 4-6 Hz frequency band for resting tremor and around 7-11 Hz for postural/kinetic tremor [13]. The power of the smoothed sEMG was found to be concentrated in 0-40 Hz range. Measures such as the frequency with maximum power over the tremor band and the mean frequency were calculated to provide predictive information related to tremor. The power spectral density of smoothed sEMG was calculated over 1-second windows using 512-point Fourier transform. This gives the power P_k of the signal at frequency bands centered around f_k, $k \in \{1, ..., N\}$ where $f_N - f_1$ is the signal bandwidth. We omit the 0-3 Hz band which contain the DC component and very low frequency movement artifacts. Since the power of patient-specific tremor frequency in 4-10 Hz band is expected to increase at the onset of tremor, we calculate F_{max}, the frequency with maximum power (P_{max}) in this frequency range of our interest, $f_B - f_1$ where f_1 is 4 Hz, f_B is 10 Hz, f_N is 40 Hz, B=7 and N=36. The index ($j^\star$) of the frequency with maximum power ($f_j^\star$) is defined as:

$$j^\star = \arg \max_{j \in \{1,...,B\}} \{P_j\}, \tag{3.1}$$

and the power (P_{max}) at peak frequency (F_{max}) is defined as

$$P_{\text{max}} = \frac{P_{j^\star}}{\sum_{j\in\{B+1,\ldots,N\}} P_j}, \tag{3.2}$$

$$F_{\text{max}} = f_{j^\star} \tag{3.3}$$

P_{max} is normalized by the power outside the bandwidth of interest so the power is comparable over different trials. This metric in (Equation 3.2) can be interpreted as the signal-to-noise ratio.

Relative power (P_{rel}) was also calculated to measure the total shift of power towards the 4-10 Hz band using the following:

$$P_{\text{rel}} = \frac{\sum_{j\in\{1,\ldots,B\}} P_j}{\sum_{j\in\{1,\ldots,N\}} P_j}, \tag{3.4}$$

The mean frequency gives the expected frequency over the spectrum of 3-40 Hz and is given as:

$$F_{\text{mean}} = \frac{\sum_{k=1}^{N} f_k P_k}{\sum_{k=1}^{N} P_k}. \tag{3.5}$$

Wavelet analysis was also carried out to calculate mean power of the signal in its wavelet bands. Using Daubechies4 discrete wavelet transform (DWT), the sEMG signal was decomposed into M=10 bands. The signal component in the j-th frequency band, $j \in \{1, ..., M\}$ is given as $x_j(t)$ over a window of ΔT = 1 s. Mean power of $x_j(t)$ is calculated as:

$$\overline{P_j} = \frac{1}{\Delta T} \sum_{t \in \Delta T} |x_j(t)|^2 \tag{3.6}$$

These spectral measures were also calculated for the acc signal.

3.1.2 Entropy measures

Wavelet Entropy (WtEn) was calculated to measure the degree of disorder based on the normalized power in different wavelet bands of the smoothed sEMG. The normalized power of $x_j(t)$ can be treated as a probability mass function for calculating WtEn and is given as:

$$p_j(t) = \frac{|x_j(t)|^2}{\sum_{k=1}^{M} |x_k(t)|^2},\ j \in \{1, ..., M\} \tag{3.7}$$

Using the definition of entropy, WtEn can be computed as:

$$H_{\text{wt}}(t) = \sum_{j=1}^{M} p_j(t) \log \frac{1}{p_j(t)} \tag{3.8}$$

For a periodic signal, value of WtEn will be low since the normalized power is concentrated in one of the wavelet levels and a limited power is contained in the remaining wavelet levels. In contrast, for a disorderly signal, WtEn will be high as there will be significant contributions from all the wavelet bands.

Sample entropy was calculated for assessing the complexity of the smoothed sEMG signal. This metric evaluates self-similarity of a data series and is calculated as the negative logarithm of the conditional probability that two sub-sequences of the series of a given length that match within a given

tolerance also match when the length is increased by one. Given these parameters of similarity tolerance criterion, r, and the pattern length of the sub-sequence, m, we can compute the sample entropy of a series $U = \{x(i),\ i \in \{1, ..., L\}\}$ where L is its length. A set of sequences of U of pattern length m was constructed and is given as $\mathbf{x}_m(i) = [x(i), ..., x(i + m - 1)]$ for $i \in \{1, ..., L - m + 1\}$. The ℓ_∞ distance between two sequences $\mathbf{x}(i)$ and $\mathbf{x}(j)$ was calculated as:

$$d_\infty[\mathbf{x}(i), \mathbf{x}(j)] = \max_{k \in \{1,...,m\}} |x(i + k - 1) - x(j + k - 1)|.$$

For the created sequences in the set, we find the matches within the similarity criterion as:

$$B_i^m(r) = |\{j :\ d_\infty[\mathbf{x}_m(i), \mathbf{x}_m(j)] \leq r\}| \tag{3.9}$$

for $i, j \in \{1, ..., L - m\}, i \neq j$. Self-matches are not considered in Sample entropy, unlike approximate entropy where lower values may be be obtained due to self-matches leading to signals being interpreted as more regular than they are. Let

$$B^m(r) = \sum_{i=1}^{L-m} B_i^m(r), \quad B^{m+1}(r) = \sum_{i=1}^{L-m} B_i^{m+1}(r). \tag{3.10}$$

The sample entropy, SpEn(U, m, r), is then defined as:

$$\text{SpEn}(U, m, r) = \lim_{L \to \infty} -\log \frac{B^{m+1}(r)}{B^m(r)}. \tag{3.11}$$

A lower SpEn(U, m, r) value reflects more self-similarity in the series and therefore, a high degree of regularity. Parameter values of pattern length and tolerance were taken as $m = 3$ and $r = 0.15\sigma$.

3.1.3 Recurrence Quantification Analysis (RQA)

RQA analysis of sEMG was performed to assess motor unit synchronization. It has been extensively used for analysis of sEMG for detecting hidden characteristics that cannot be detected by linear analysis [39,40]. This nonlinear method measures the complexity of a time series by quantifying the number and duration of recurrences presented by the phase space trajectory of the dynamic system. The recurrence rate is calculated as the density of recurring point in the recurrence plot.

Recurrence plot or recurrence matrix (RM) for the series U was computed as follows:

$$R_{i,j} = \Theta(r - \|\mathbf{x}_i - \mathbf{x}_j\|),\ (i,j) \in \{1, ..., L - (M-1)\tau\} \tag{3.12}$$

where, $\mathbf{x}_i = [x(i), x(i+\tau), ..., x(i+(m-1)\tau)]$ for $i \in \{1, ..., L - (M-1)\}$ is a vector of length m, $\|\cdot\|$ is the Euclidean norm, r is the radius, Θ is the Heaviside function, M is the embedding dimension, τ is the time delay, and L is the length of the time series U.

From $R_{i,j}$, the recurrence rate R is calculated as:

$$\mathsf{R} = \frac{1}{P^2} \sum_{i,j} R_{i,j}. \tag{3.13}$$

R is more sensitive to changes in the degree of synchronization than linear variables such as mean/median frequency [40].

We used $M = 5,\ \tau = 3, r = 0.33,\ L = 1000$ as described in [41].

3.2 Machine Learning Algorithms

In [22], a manual algorithm was used for the design of a closed-loop DBS system. The process of setting the thresholds manually for different parameters to predict the advent of tremor can be challenging. A Back-propagation neural network (BPNN) was used to automate the process as described in [32] for 2 PD patients but was unable to achieve 100% sensitivity. Another neural network, LNN-1, was proposed for tremor prediction in [34]. Preliminary results of training LNN-1 with data from 1 patient showed that it performed better than the BPNN. Here, we present the set-ups of automated tremor prediction algorithms using DT and modified version of LNN-1 i.e. LNN-2. We used the same set of features for both the algorithms. Training and testing data consisted of these attributes for each trial after the stimulation was switched off to the End of File (EOF). Detailed description of each of the algorithms is given in this section.

3.2.1 Modified LAMSTAR Neural network

LArge Memory STorage and Retrieval neural network, as the name suggests, can store and retrieve a large number of patterns. The classic setup of this neural network is based on the concepts of Kohonen's Self-organizing map (SOM) and Hebbian learning. Figure 4 shows the structure of LNN comprising of 9 SOM layers and one output layer. LNN input "word" consists of attributes or "subwords" extracted from sEMG and Acc. Here, an instance of feature set used for prediction algorithm is shown. The attributes are fed to their respective SOM layer. Each layer i consists of N_i neurons. A representative example of winner neurons for a given set of SOM layers is shown. The shaded boxes represent the winner neurons at a time instant. Each of the N_i neurons in each SOM layer are connected to the output

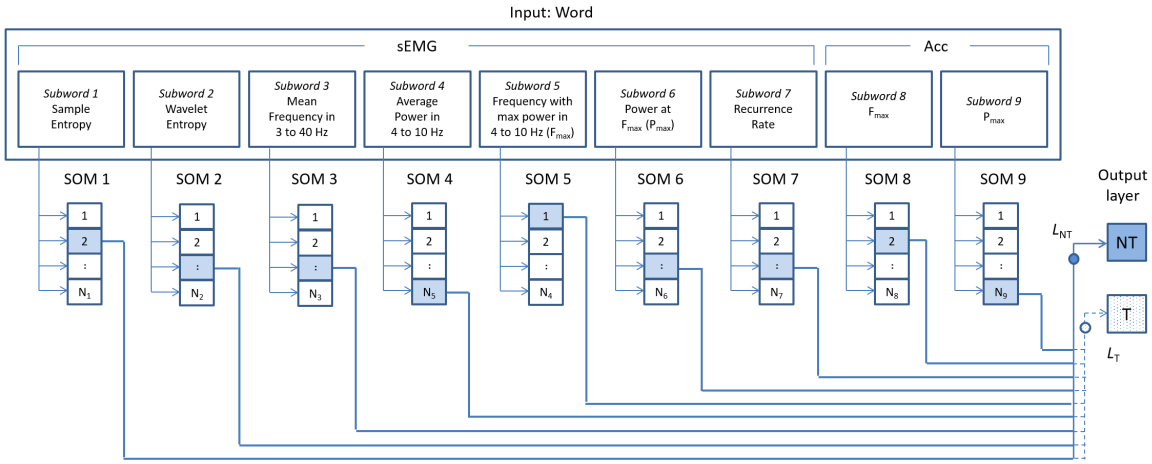

Figure 4. Architecture of LNN consisting of self-organizing maps and output layer connected by link weights that update based on Hebbian learning

layer via Link weights. Link from winner neuron of each layer to output neuron related to the event of "No tremor" (NT) or "Tremor" (T) are rewarded or punished. The weight of these links represent the strength of associations between the neurons, similar to synaptic weights in the nervous system. Output NT or T is decided by comparing the sum of link weights from the winner neurons to the output neurons, $\sum L_{NT}$ and $\sum L_T$ respectively normalized by the number of times a neuron activates in association with NT or T. Output neuron corresponding to greater of the sums of mormalized link weights wins. We first describe the Winner-Take-All (WTA) layers in this setup, followed by the supervised link weight update.

The input to this network is called a "word", consisting of an instance of the feature set. Each word is split into subwords that are fed to separate SOM layers. For the eight PD and four ET patients, 8-12 features were selected from the extracted set corresponding to 8-12 layers. These SOM layers contain

a fixed number of neurons and follow Winner-Take-All (WTA) principle i.e. only one neuron in each SOM layer will fire for a given instance of data. SOM is an unsupervised method used for clustering where the winner of each module is determined by finding the neuron with minimum distance from a given input vector. The number of neurons can be predetermined or set dynamically, thus dividing the feature space into different regions. The binning of these WTA layers can also be performed by other discretizing methods than the conventional SOM binning. These include unsupervised methods such as equal width, equal frequency and supervised methods that use entropy or other metrics to create bins. Minimum Description Length (MDL), a supervised method, is used in this setup since the dataset is small and unsupervised clustering method may not give the optimal boundaries. Class information entropy is used for selection of boundaries. It is a top-down method that starts with one interval and keeps splitting till the criterion is met. The method is given in detail in [42]. For attributes where no partition cut point satisfied the MDL criterion, equal frequency or equal width method was used to create 3-8 bins or neurons.

As shown in the Figure 4, each neuron of each SOM layer is connected to each neuron of the output layer via link weights (L_{NT} or L_T). According to Hebbs rule, if for a set of inputs, certain elements are activated, then by repeated occurrence of these patterns, the activated elements get increasingly strongly associated. For LNN training, these link weights are updated in a supervised manner, either rewarded or punished based on the output class. These links can be treated as synapses of a neuronal network whose weights increase in a Hebbian manner. This update occurs for the link weights from only the winner neurons of all SOM layers. At time $t + 1$, the link weights at previous time t from the winning neuron w of each module k to the winning decision neuron v are rewarded by ΔL. Link weights from

the winning neuron w of each layer k to all the other non-winning decision neurons j are punished by ΔM. Following are the equations for reward and punishment of the link weights:

$$L^k_{w,v}(t+1) = L^k_{w,v}(t) + \Delta L, \tag{3.14}$$

$$L^k_{w,j}(t+1) = L^k_{w,j}(t) - \Delta M \tag{3.15}$$

When a neuron of a layer fires, the link-weight from this winner neuron to the output neuron of the corresponding class, gets rewarded as in (Equation 3.14). Rest of the link-weights from this winner neuron, get punished as in (Equation 3.15).

Finally, the predicted class is the one with maximum value of the sum of link weights from the winner neurons to each output class neuron. A variation of LNN, known as modified or normalized LAMSTAR, is used here. In case of modified LNN, denoted as LNN-2, the link weights are normalized with respect to the number of times a winner neuron has fired with an associated decision neuron. The number of times a winner neuron w was activated with an associated decision neuron i is given by $n^k_{w,i}$. The link weights are normalized as given below:

$$L^k_{w,i}{}^* = \frac{L^k_{w,i}}{n^k_{w,i}} \tag{3.16}$$

The decision for LNN-2 with K layers and J output neurons, is given by the following equation:

$$\sum_{k \in K} L^k_{w,v}{}^* > \sum_{k \in K} L^k_{w,j}{}^*, \forall j \in J, j \neq v \tag{3.17}$$

Normalization of link weights, as in LNN-2, has been reported to improve the results compared to the classic LNN setup (LNN-1) [37, 38]. This is especially beneficial in case of unbalanced datasets such as in our case where number of tremor onset datapoints are limited compared to the data where no tremor was observed.

3.2.2 Decision Tree Learning

Decision tree model is a popular technique used to produce a set of tree-based rules. The decision tree consists of nodes and leaves where each node represents a condition or rule on an attribute, and the leaves or the terminal nodes signify the decision. This algorithm is trained in a greedy manner by finding the optimal local solution based on Gini impurity of the features for splitting the data. Starting with the root node, the tree is built by recursively dividing the data into smaller subsets using the feature and its split criterion that gives the least node impurity. At each level, node n is divided into right node n_r and left node n_l. The process is recursively carried out till a condition is met, either all the data is classified or till the maximum number of levels are reached. At each level, the descendant subsets are 'purer' than the parent dataset and contain majority of one class. This method of space partitioning creates hyper-rectangles and these hyperspaces represent different categories. Gini impurity, the metric used for measuring impurity at each node n, is given as:

$$i(n) = 1 - \sum_{k=1}^{K} p(k|n)^2. \tag{3.18}$$

where K is the total number of decision categories and $p(k|n)$ is the proportion of class k at the node n. The split leads to decrease in impurity, $\Delta i(s, n) = i(n) - p_l i(n_l) - p_r i(n_r)$ where p_l and p_r are the

proportions of classes in left and right nodes, respectively and s is the split threshold applied to the node n. $\Delta i(n)$ gives the measure of goodness of split' and is maximized by selection of the best split. The best split criterion is obtained by selecting the split s^* giving the largest decrease in impurity, given by:

$$\Delta i(s^*, n_R) = \max_{s \in S} \Delta i(s, n_R) \tag{3.19}$$

In the designed tremor prediction algorithm, DT makes the decision of either tremor predicted or tremor not predicted, denoted as T and NT, respectively. The number of categories is $K = 2$. The tree can then be pruned to avoid overfitting for the given training data. This step is especially useful for sparse or high-dimensional dataset.

3.2.3 Minimax Support Vector Machine

Previously, a Support Vector Machine (SVM) algorithm was also compared to DT with DT performing better. An SVM is suitable for binary classification where an optimal hyperplane is found such that the data is separated by maximum margin. In this work, we used a variation of SVM which uses minimax hinge loss instead of 0-1 loss or hinge loss functions. Figure 5 shows the different loss functions [43]. Minimax hinge-loss is as following, given α^* the optimal linear predictor for n samples (x_i, y_i):

$$\min_{\alpha} \frac{1}{n} \sum_{k \in 1:n} max(0, \frac{1 - y_i \alpha^T x_i}{2}, y_i \alpha^T x_i) + \epsilon ||\alpha|| \tag{3.20}$$

In this approach, the minimax hinge loss SVM is implemented by applying sub-gradient descent to obtain the parameters of the SVM model.

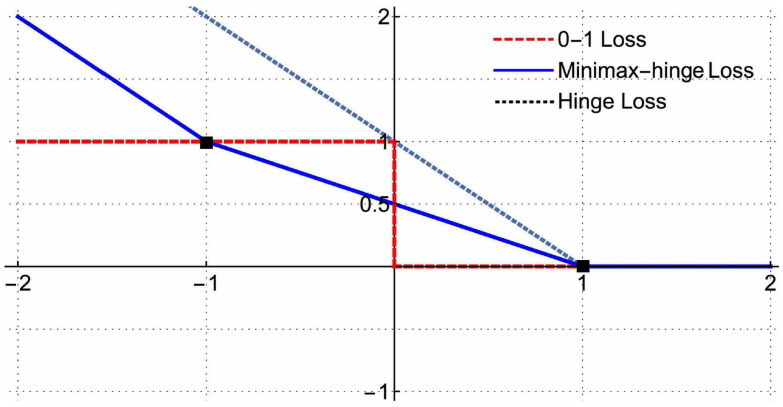

Figure 5. Minimax hinge loss vs 0-1 loss and Hinge loss

3.3 Performance metrics

We define the metrics of accuracy, sensitivity and β ratio to best reflect the performance of the algorithms. Figure 6 shows a trial where tremor was observed. Typical events noted during a recording trial include:

1. time when stimulation is switched: t_{on},
2. time when stimulation is stopped: t_{s},
3. time when tremor is observed: t_{o}, and
4. time where recording is stopped or end-of-file: t_{EOF}.

Tremor correctly predicted at time t_{p} is showed as an example of $True\ Positive$ or TP prediction in second row of Figure 6. Examples of early prediction and late prediction for the given trial are shown as

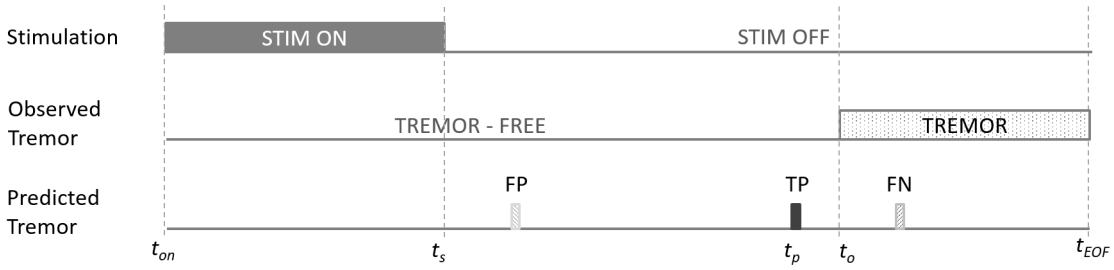

Figure 6. Definitions of TP, TN, FP and FN for tremor prediction using machine learning algorithms

the gray blocks in the third series, indicated as FP and FN, respectively, representing $False\ Positive$ and $False\ Negative$. The algorithms check for onset of tremor only after the stimulation is switched off at time t_{s}. The actual tremor is observed at time t_{o}.

If the tremor onset is predicted in the second half of the duration from t_{s} to t_{o}, we say that tremor was correctly predicted and define this trial as a $True\ Positive$ or TP. If the prediction is made in the first half of the duration of t_{s} to t_{o}, the prediction is too early and is classified as $False\ Positive$ or FP. This way, we can penalize early prediction which are not helpful for an effective closed-loop system. We allow prediction in less than 1 s of tremor being observed. If the tremor is predicted beyond 1 s of tremor being detected, then the prediction is too late and is defined as $False\ Negative$ or FN. In cases where no tremor is observed till the EOF and tremor is not predicted till this time t_{EOF}, the trial is classified as $True\ Negative$ or TN.

Based on these definitions of TP, TN, FP and FN, we give the performance metrics as follows:

$$\mathsf{Accuracy(A)} = \frac{\#TP + \#TN}{\#TP + \#TN + \#FP + \#FN} \tag{3.21}$$

$$\mathsf{Sensitivity(S)} = \frac{\#TP}{\#TP + \#FN} \tag{3.22}$$

The sensitivity needs to be 100% so that the patient does not experience tremor when the stimulation is switched off. Accuracy, which gives the ratio of correct predictions to total number of trials should be high. These metrics do not give information about how close the prediction is made to the actual observed tremor. Therefore, we defined ratios R_{o}, R_{p} and β to assess the performance of algorithms with respect to how good the prediction is.

$$R_{\mathrm{o}} = \sum(t_{\mathrm{o}} - t_{\mathrm{s}}) / \sum(t_{\mathrm{s}} - t_{\mathrm{on}}), \tag{3.23}$$

$$R_{\mathrm{p}} = \sum(t_{\mathrm{p}} - t_{\mathrm{s}}) / \sum(t_{\mathrm{s}} - t_{\mathrm{on}}), \tag{3.24}$$

$$\beta = \sum(t_{\mathrm{p}} - t_{\mathrm{s}}) / \sum(t_{\mathrm{o}} - t_{\mathrm{s}}) \tag{3.25}$$

R_{o} gives the ratio of observed tremor-free time to the duration of stimulation. R_{p} gives a similar ratio for predicted delay in tremor. In the trials where tremor was not observed till EOF, we can consider t_{EOF} - t_{s} as the tremor-free time. R_{o} is then calculated as the ratio of this tremor-free period to the duration of stimulation. β is the ratio of R_{p} to R_{o}, giving a measure of prediction performance. Closer the number

is to 1, closer the prediction is made to the observed tremor. Average across patients was calculated based on the number of trials in that patient.

Percentage of observed and predicted stimulation-free time are given by $P_{\text{sf\_o}}$ (%) and $P_{\text{sf\_p}}$ (%), respectively.

$$P_{\text{sf\_o}}(\%) = \frac{R_{\text{o}}}{1 + R_{\text{o}}}.100 \tag{3.26}$$

$$P_{\text{sf\_p}}(\%) = \frac{R_{\text{p}}}{1 + R_{\text{p}}}.100 \tag{3.27}$$

For example, if R_{o} is equal to 4, stimulation can be off for 80% of the total time. The effective percentage of battery power that can be saved is $P_{\text{sf\_p}}$ for the actual closed-loop tremor prediction system. Weighted average for a performance metric is given as $\sum_{i \in 1,..,8}(n_i.M_i)/\sum_{i \in 1,..,8}(n_i)$ where n_i is the number of test trials and M_i is the performance metric for patient i.

CHAPTER 4

COMPARISON OF PERFORMANCE OF TREMOR PREDICTION ALGORITHMS

Results from this section to be submitted for publication.

4.1 Tremor prediction results

Performance of tremor predition algorithms is evaluated here where the algorithms are trained in offline learning mode such that the algorithm parameters are set during the training phase and remain unchanged during the testing phase. For the patients with two sessions of recordings, trials from the same session were used for training and testing. LNN-2 and DT were run for all states combined as well as for state-specific mode. Both the algorithms did not perform as well for when trained for all states together, giving early predictions and low β ratio. This is expected since the movement action could be misclassified as tremor onset. When trained for all states, tremor onset may also be misinterpreted as action, leading to low sensitivity. Rest of the results are presented for algorithms when trained for state-specific mode. This initial separation of action from posture and rest states lead to higher β ratio and sensitivity. Following are exemplars of features used and the resulting cases of TP, FP and TN.

Figure 7 – Figure 10 show set of sEMG and acc based features for TP, FP, and TN cases during Rest, Action and Posture states. Same set of features were used for training of both DT and LNN-2 for fair comparison. Figure 7 displays a resting state trial with stimulation duration of 30 s. Smoothed extensor sEMG and its sample entropy are given in top two rows, and power in 4-10 Hz of accelerometer signal with raw triaxial accelerometer signals are shown in bottom two rows. Black dot-

dashed line shows where the stimulation was switched off, red line indicates where tremor was actually observed. The tremor was observed at 250 s giving a high R_{o} ratio of 6.45. LNN-2 correctly recognizes onset of tremor within 1 s of actual reappearance of tremor. Gray line indicates where DT made an early prediction for state-specific training and dashed blue line shows where tremor was correctly predicted by LNN-2 for separately training Action and Posture/Rest modes.

Figure 8 shows the drop in sEMG sample entropy and an increase in accelerometer power in 4-10 Hz at 250 s of this same trial when tremor reappears after switching off the stimulation in previous "rest" trial. Both these parameters indicate the start of periodic tremor oscillations. Raw acc signal shows prominent tremor oscillations which is reflected by the increase of acc power in 4-10 Hz. Red vertical line indicates observed tremor and dashed blue line indicates tremor "prediction" by LNN-2. The delay in "prediction of tremor" is by 0.5 s which is acceptable since the onset of tremor is just setting in. DT predicts the tremor earlier at 151 s but with a high R_{p} of 2.97. Small oscillations are seen in the accelerometer signals; however, a corresponding drop in sample entropy or increase in acc 4-10 Hz power was not observed at this time. This was also classified as TP.

Figure 9 shows Smoothed sEMG, its sample entropy and recurrence rate during an Action state trial with stimulation duration of 50 s. Green dashed line shows start of voluntary movement, black dot-dashed line indicates stimulation "off" time and red line shows the time when tremor was observed. Gray and Dashed blue line show comparison between training for combined states vs training separately for the states. An early prediction (FP) was made by both DT and LNN-2 when they were trained for the Action, Posture and Rest states together. Early prediction, shown by the gray line, may be due to mistaking movement as tremor onset ($False\ Positive$). When "Action" files are trained separately,

both DT and LNN2 correctly identify onset of tremor around a second prior than when the tremor was actually observed ($True\ Positive$). Prediction was made at 69.75 s and 69 s, with a β of 0.98 and 0.94, by DT and LNN-2, respectively. .

An exemplar of TN is illustrated in Figure 10. Smoothed extensor sEMG and features extracted from this signal, namely, sample entropy and power in 4-10 Hz, are given for a trial during "Posture" mode (stim duration = 30 s). Green dashed line indicates the start of voluntary movement and black dot-dashed line shows where the stimulation was switched off. In this trial of "Posture" state (stimulation duration of 30 s), no tremor was observed even after 120 s of stimulation being switched off. Postural movement was initiated at 58.5 s and some movement can be observed in the acc signal. Both DT and LNN-2, when trained for all states together as well as for state-specific training, accurately, did not predict tremor till the EOF. Accelerometer signals are also shown in the bottom row for x, y and z axes.

4.1.1 PD

Comparison of LNN-2 and DT performance metrics is shown in Table IV for PD patients for all DS. The total number of trials (N_{to}), the number of training trials (N_{tr}) and that for testing (N_{te}) are listed as well. For each PD patient, 65-75% of total files were used for training the algorithms. Both the algorithms were trained separately for Action and Posture / Rest states. A and S columns give the accuracy and sensitivity (%) achieved by DT and LNN-2 for each patient. Bottom rows give the total number of files, total number of TP, TN, FP and FN, along with weighted average of accuracy and sensitivity (%) across all PD patients. LNN-2 performs better with sensitivity of 100%. For trials at all DS, sensitivity of DT is not 100% due to one FN. The total number of files for PD7 is 9; however, only 2 of the files were in action mode. This made training for action mode separately not feasible for this

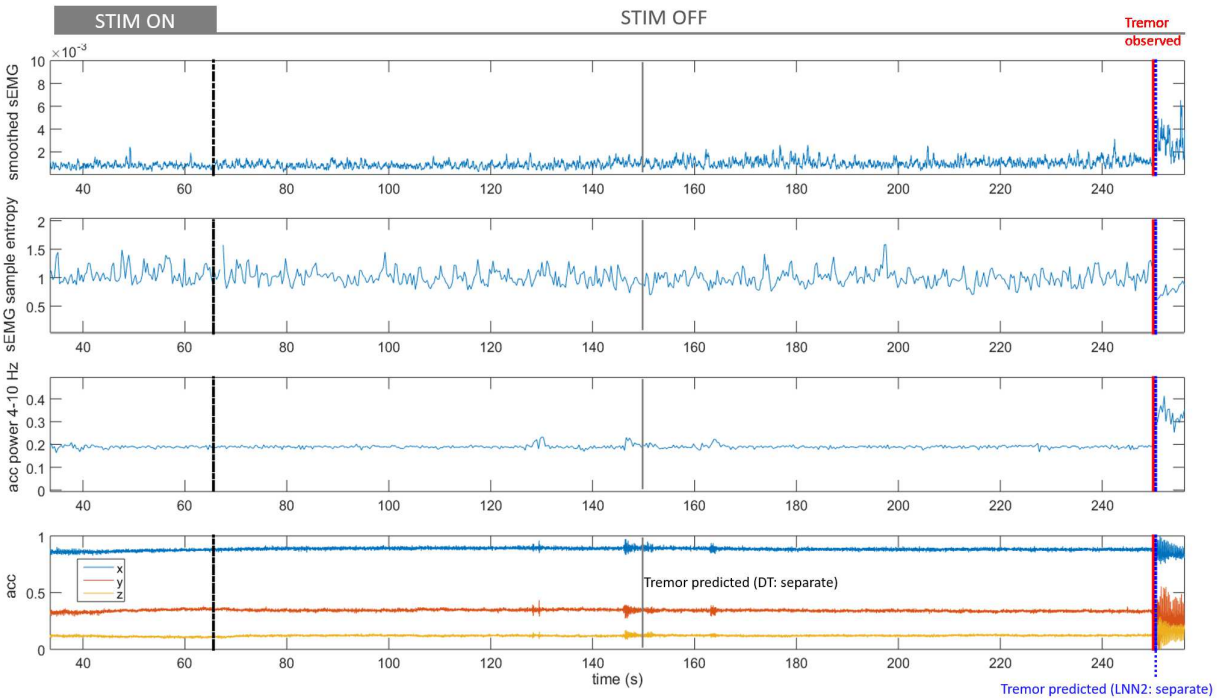

Figure 7. A "Rest" trial (stim duration = 30 s) with $True\ Positive$ prediction

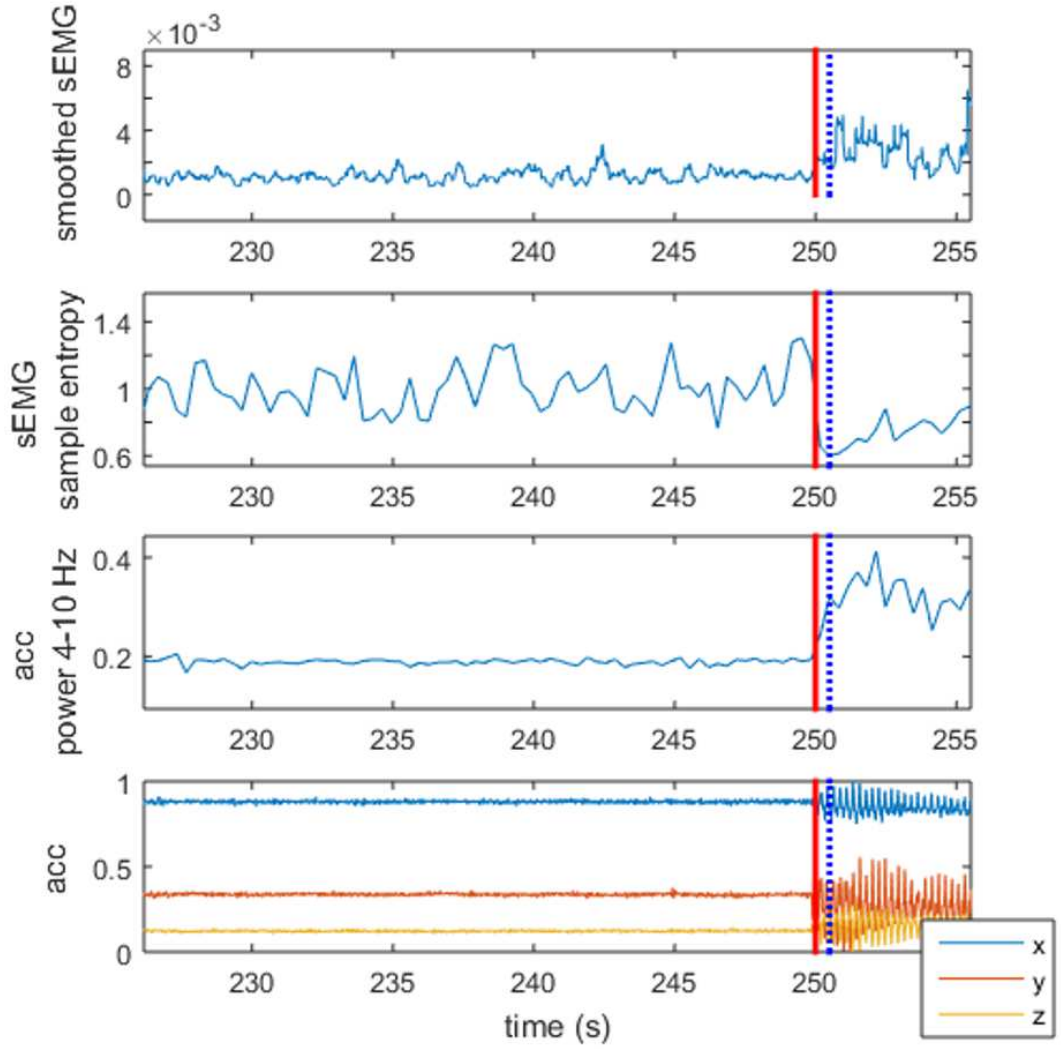

Figure 8. Zoomed-in plot of sEMG and acc features for “Rest” trial with $True\ Positive$ prediction

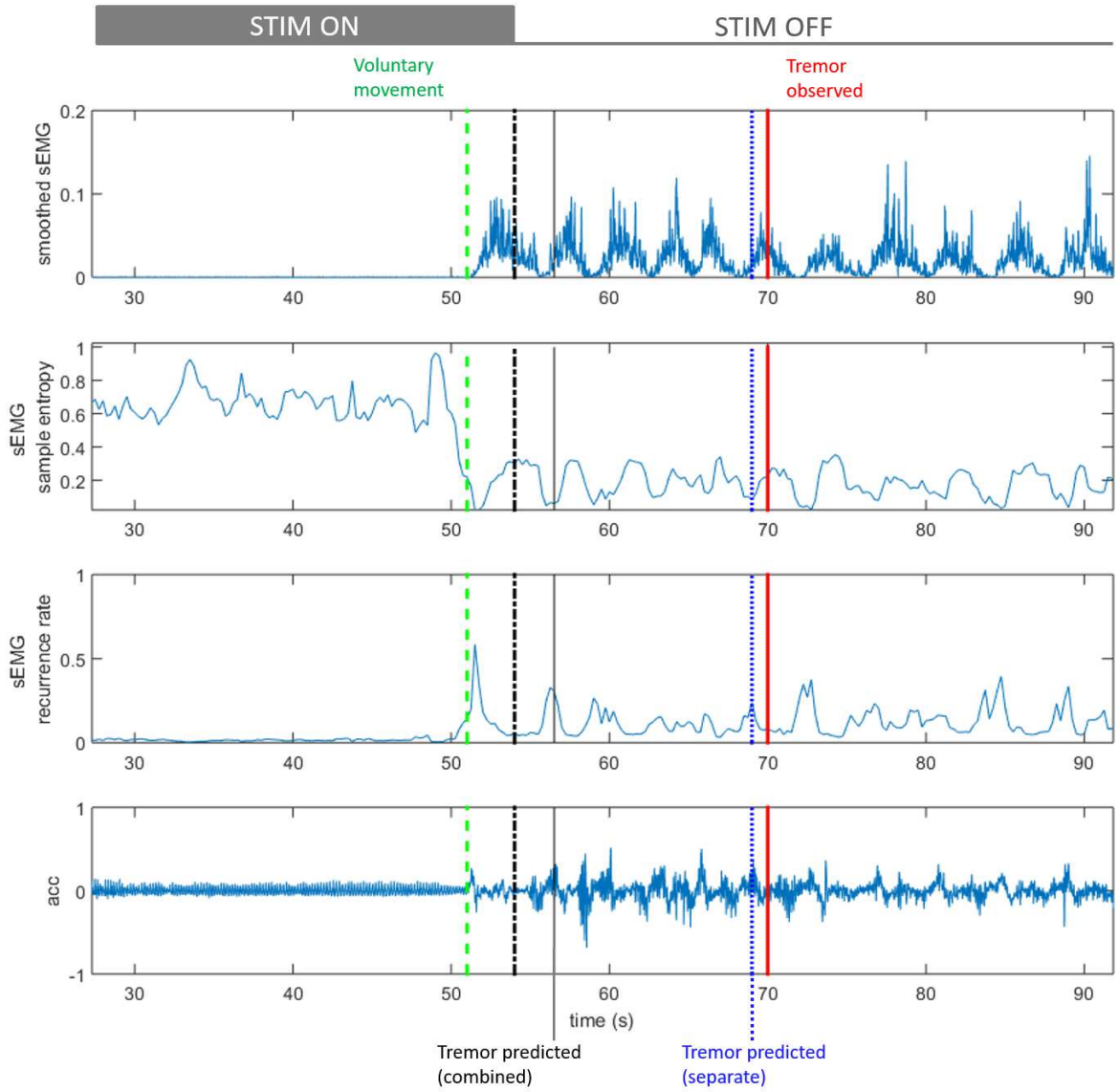

Figure 9. An "Action" trial (stim duration = 50 s) with $True\ Positive$ prediction (separate modes) and $False\ Positive$ prediction (combined modes)

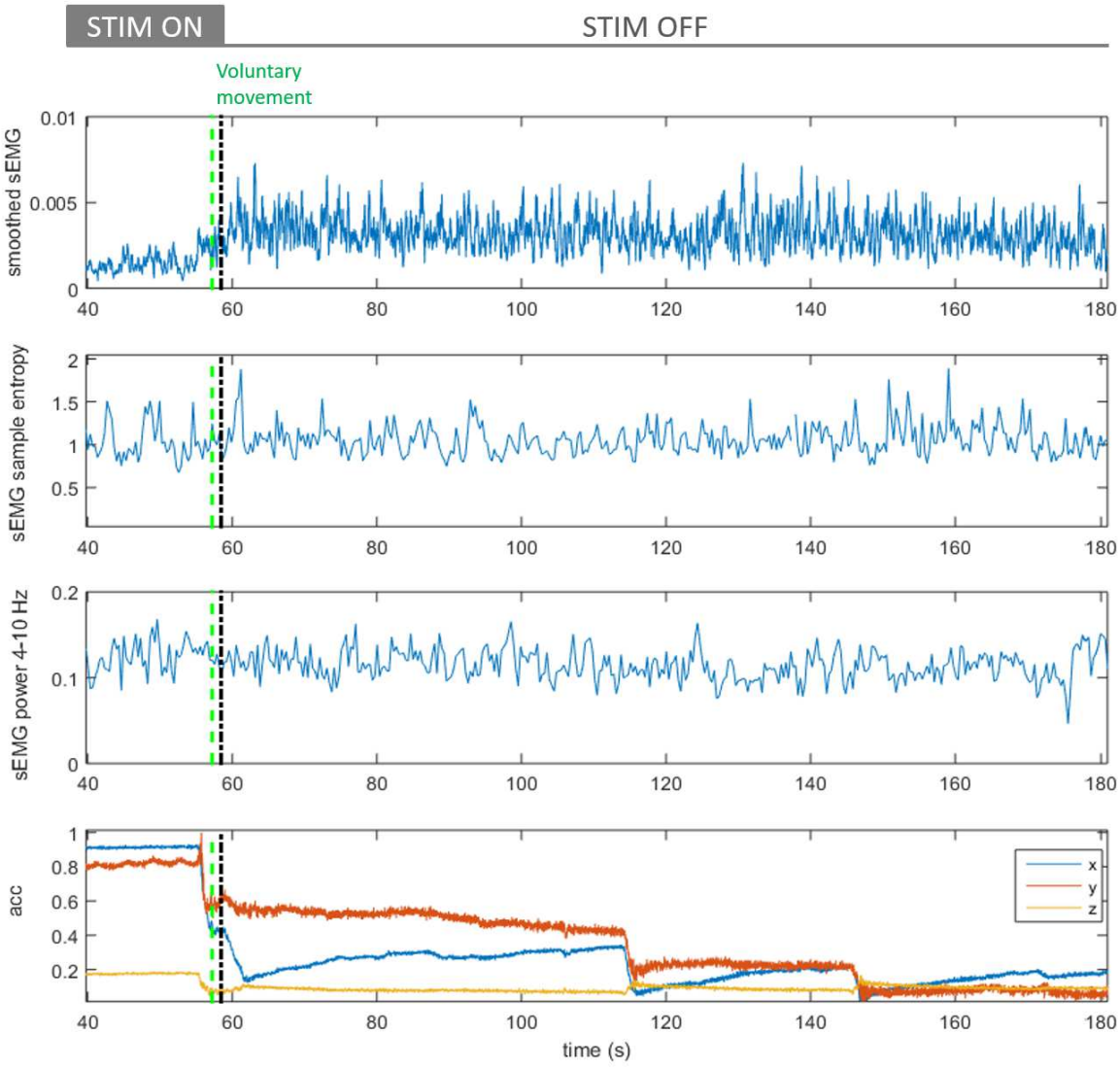

Figure 10. A "Posture" trial (stim duration = 30 s) with $True\ Negative$ prediction

patient, leading to only the posture/rest files to be used. Therefore, the total number of files are given to be 7 for PD7.

Table V give the observed and predicted R-ratios for state-specific training of DT and LNN-2. R_o gives the ratio of duration of observed tremor free time from the time stimulation was switched off to the duration of stimulation applied. This ratio is given for all trials and the test trials for each patient. R_p gives the ratio of duration of predicted tremor free time from the stimulation "off" time to the duration of stimulation. Lower the difference between R_p and R_o, closer the prediction of tremor is to the actual observed tremor. DT R_{p} and LNN-2 R_{p}, calculated over N_{te} trials for each patient, are compared to the R_{o} of those N_{te} trials.

β is the ratio of the predicted tremor free time (R_p) to the observed tremor free time (R_o) from the time stimulation was switched off. Closer this value is to 1, closer the prediction of tremor is to the actual observed tremor. β of PD7 is greater than one but since the tremor onset is predicted within one second of observed tremor, we accept these as correct recognitions. The weighted average is calculated with respect to the number of trials. R_p ratio is also expressed in terms of percentage of stimulation-free time P_{sf-p} (%). R_o ratio based P_{sf-p} (%) gives the maximum possible percentage of stimulation-free time. P_{sf-p} (%) represents the average feasible percentage of stimulation-free time using the tremor prediction algorithms. Overall the ratio R_{p} and $P_{sf-p}\%$ are higher for LNN-2 than for DT.

The performance of LNN-2 and DT was also compared with minimax SVM. However, the minimax SVM classifier did not perform well and had a low weighted average β value of 0.72, and accuracy and sensitivity of 75% and 79%, respectively, for the 47 PD patient trials.

TABLE IV. Performance of DT and LNN-2 for tremor prediction in eight PD patients when the algorithms were trained separately for the states of Action and Posture/Rest. The number of total trials (N_{to}), the number of training trials (N_{tr}) and the number trials used for testing (N_{te}) are given for each patient. TP, TN, FP and FN give the True Positive, True Negative, False Positive and False Negative, respectively. A and S columns give the accuracy and sensitivity (%) achieved by DT and LNN-2 for each patient. The weighted average is calculated with respect to the number of trials. For PD7*, number of 'Action' files were limited to train DT and LNN-2 separately for the state.

Patient	**Performance comparison between DT and LNN-2**														
	N_{to}	N_{tr}	N_{te}	**DT**						**LNN-2**					
				TP	**TN**	**FP**	**FN**	A **(%)**	S **(%)**	**TP**	**TN**	**FP**	**FN**	A **(%)**	S **(%)**
PD1	16	11	5	4	0	1	0	80.00	100.00	5	0	0	0	100.00	100.00
PD2	26	17	9	5	1	2	1	66.67	83.33	5	1	3	0	66.67	100.00
PD3	17	12	5	5	0	0	0	100.00	100.00	5	0	0	0	100.00	100.00
PD4	32	23	9	4	3	2	0	77.78	100.00	4	3	2	0	77.78	100.00
PD5	20	13	7	7	0	0	0	100.00	100.00	6	0	1	0	85.71	100.00
PD6	29	23	6	5	1	0	0	100.00	100.00	5	1	0	0	100.00	100.00
PD7*	7	5	2	2	0	0	0	100.00	100.00	2	0	0	0	100.00	100.00
PD8	14	10	4	3	1	0	0	100.00	100.00	3	1	0	0	100.00	100.00
Total	**161**	**114**	**47**	**35**	**6**	**5**	**1**			**35**	**6**	**6**	**0**		
Wt Avg								**87.23**	**91.67**					**87.23**	**100.00**

TABLE V. R-ratios obtained using DT and LNN-2 in eight PD patients when the algorithms were trained separately for the states of Action and Posture/Rest. R_o gives the ratio of duration of observed tremor free time from the time stimulation was switched off to the duration of stimulation applied. This ratio is given for all trials and the test trials for each patient. R_p gives the ratio of duration of predicted tremor free time from the stimulation "off" time to the duration of stimulation. β is the ratio of the predicted tremor free time (R_p) to the observed tremor free time (R_o) from the time stimulation was switched off. Closer this value is to 1, closer the prediction of tremor is to the actual observed tremor. For PD7*, number of 'Action' files were limited to train DT and LNN-2 separately for the state. Tremor was predicted within 1 second of tremor onset, giving $R_p > R_o$

Patient	**R-ratio comparison between DT and LNN-2**										
	All trials		**Test trials**								
						DT			**LNN-2**		
	N_{to}	R_o	N_{te}	R_o	P_{sf-o}**%**	R_p	β	P_{sf-p}**%**	R_p	β	P_{sf-p}**%**
PD1	16	0.52	5	0.40	28.57	0.29	0.75	22.48	0.30	0.77	23.07
PD2	26	0.56	9	0.75	42.86	0.53	0.71	34.64	0.50	0.67	33.33
PD3	17	0.19	5	0.15	13.04	0.12	0.83	10.71	0.12	0.82	10.71
PD4	32	0.76	9	0.86	46.24	0.69	0.81	40.83	0.72	0.84	41.86
PD5	20	0.26	7	0.21	17.36	0.20	0.95	16.67	0.20	0.95	16.67
PD6	29	3.53	6	2.79	73.61	2.24	0.80	69.1	2.73	0.94	73.19
PD7*	7	0.41	2	0.32	24.24	0.33	1.03	24.81	0.34	1.05	25.37
PD8	14	1.71	4	2.14	68.15	2.10	0.98	67.74	2.14	1.00	68.15
Total	**161**		**47**								
Wt Avg		**1.14**		**0.95**	**48.72**	**0.79**	**0.86**	**44.13**	**0.85**	**0.88**	**45.95**

TABLE VI. Tremor prediction performance of DT and LNN-2 for test trials of eight PD patients at their optimal optimal duration of stimulation, DS*. The number of trials used for testing at DS* (N^*_{te}) are given for each patient. R^*_o and its corresponding R^*_p are noted to be higher for DS^* compared to when all the stimulation durations are considered together. β^* is the ratio of the predicted tremor free time (R^*_p) to the observed tremor free time (R^*_o) from the time stimulation was switched off. β^* of PD5 and PD7 are greater than one but since the tremor onset is predicted within one second of observed tremor, we accept these as correct recognitions. The weighted average is calculated with respect to the number of trials.

Patient	**β-ratio comparison at optimal DS***									
	Test trials at DS*									
	DS*	N^*_{te}	R^*_o	P^*_{sf-o}**%**	**DT**			**LNN-2**		
					R^*_p	β^*	P^*_{sf-p}**%**	R^*_p	β^*	P^*_{sf-p}**%**
PD1	30	3	0.38	27.54	0.31	0.81	23.66	0.33	0.86	24.81
PD2	20	3	0.87	46.52	0.69	0.79	40.83	0.70	0.80	41.18
PD3	NA	-	-	-	-	-	-	-	-	
PD4	20	3	1.18	54.13	0.96	0.81	48.98	1.21	0.95	52.83
PD5	30	1	0.43	30.07	0.47	1.08	31.97	0.42	0.97	29.58
PD6	30	4	3.80	79.17	2.80	0.81	73.68	3.68	0.97	78.63
PD7*	30	1	0.50	33.33	0.51	1.02	33.77	0.51	1.02	33.77
PD8	30	4	2.34	70.06	2.31	0.98	69.79	2.34	1.00	70.06
Total		**19**								
Wt Avg			**1.73**	**63.37**	**1.44**	**0.89**	**59.02**	**1.66**	**0.94**	**62.41**

LNN-2 and DT performance are also compared for trials at DS^* only in Table VI. These ratios are given only for the trials of optimal duration of stimulation (DS^*) along with the DS^* for that patient. The number trials used for testing at DS^* (N^*_{te}) are given for each patient. R^*_o and its corresponding R^*_p are noted to be higher for DS^* compared to when all the stimulation durations are considered together. β^* is the ratio of the predicted tremor free time (R_p) to the observed tremor free time (R_o) from the time stimulation was switched off. Closer this value is to 1, closer the prediction of tremor is to the actual observed tremor. β^* of PD5 and PD7 are greater than one but since the tremor onset is predicted within one second of observed tremor, we accept these as correct recognitions. The weighted average is calculated with respect to the number of trials. For trials at DS^*, the accuracy and sensitivity of DT and LNN-2 are equal (100% for each patient) but the β ratio of LNN-2 (0.94) is higher than that of DT (0.89). This gives a higher stimulation-free duration percentage, which is closer to the observed P_{sf-o} at the optimal DS^*.

4.1.2 ET

Tremor prediction algorithms based on LNN-2 and DT were also run for four ET patients. Data was collected using the first set-up here. Patients performed Action and Posture tasks. ET patients do not experience tremor during Rest state; therefore, only the Action and Posture states have been considered for recording. LNN-2 and DT were trained and tested in the offline mode with no changes made to the algorithm parameters once the training phase is completed. Same set of features and the same training and testing trials were used for both the algorithms. 75-80% of all trials were used for training for each patient and the rest for testing. Performance of LNN-2 and DT is compared in Table VII and Table VIII for a total of 128 trials.

Table VII lists the total number of trials (N_{to}), the corresponding R_o, the number of testing trials (N_{te}) and the corresponding R_o for each patient. The performance metrics A and S along with TP, TN, FP and FN are given under DT and LNN-2 sections. The predicted R-ratio, R_p for test trials and their respective β values are also given for state-specific training of DT and LNN-2. Sensitivity of 100% is obtained using both the algorithms. Accuracy, and β of DT are lower than that of LNN-2. The latter algorithm performed better than DT for four ET patients in a similar manner as that observed for PD patients. A β ratio of 0.92 was obtained for LNN-2, whereas, it was 0.83 for DT, giving a higher percentage of stimulation-free duration P_{sf-p} % for LNN-2.

TABLE VII. Performance of DT and LNN-2 for tremor prediction in four ET patients when the algorithms were trained separately for the states of Action and Posture/Rest. The number of total trials (N_{to}), the number of training trials (N_{tr}) and the number trials used for testing (N_{te}) are given for each patient. TP, TN, FP and FN give the True Positive, True Negative, False Positive and False Negative, respectively. A and S columns give the accuracy and sensitivity (%) achieved by DT and LNN-2 for each patient. The weighted average is calculated with respect to the number of trials.

Patient	**Performance comparison between DT and LNN-2**														
	N_{to}	N_{tr}	N_{te}	**DT**						**LNN-2**					
				TP	**TN**	**FP**	**FN**	A **(%)**	S **(%)**	**TP**	**TN**	**FP**	**FN**	A **(%)**	S **(%)**
ET1	52	41	11	7	2	2	0	81.82	100.00	9	2	0	0	100.00	100.00
ET2	30	22	8	5	3	0	0	100.00	100.00	4	4	0	0	100.00	100.00
ET3	16	12	4	4	0	0	0	100.00	100.00	3	1	0	0	100.00	100.00
ET4	30	23	7	3	4	0	0	100.00	100.00	3	4	0	0	100.00	100.00
Total	**128**	**98**	**30**	**19**	**9**	**2**	**0**			**19**	**11**	**0**	**0**		
Wt Avg								**95.45**	**100.00**					**100.00**	**100.00**

TABLE VIII. R-ratios obtained using DT and LNN-2 in four ET patients when the algorithms were trained separately for the states of Action and Posture/Rest. R_o gives the ratio of duration of observed tremor free time from the time stimulation was switched off to the duration of stimulation applied. This ratio is given for all trials and the test trials for each patient. R_p gives the ratio of duration of predicted tremor free time from the stimulation "off" time to the duration of stimulation. β is the ratio of the predicted tremor free time (R_p) to the observed tremor free time (R_o) from the time stimulation was switched off. Closer this value is to 1, closer the prediction of tremor is to the actual observed tremor. **PD7***: Number of 'Action' files were limited to train DT and LNN-2 separately for the state. Tremor was predicted within 1 second of tremor onset, giving $R_p > R_o$

Patient	**R-ratio comparison between DT and LNN-2**										
	All trials		**Test trials**								
						DT			**LNN-2**		
	N_{to}	R_o	N_{te}	R_o	P_{sf-o}**%**	R_p	β	P_{sf-p}**%**	R_p	β	P_{sf-p}**%**
ET1	52	0.79	11	0.82	45.05	0.55	0.67	35.48	0.67	0.81	40.12
ET2	30	0.89	8	0.90	47.37	0.86	0.95	46.24	0.88	0.98	46.81
ET3	16	0.86	4	0.91	47.64	0.68	0.75	40.48	0.84	0.93	45.65
ET4	30	1.29	7	1.20	54.55	1.16	0.96	53.7	1.13	0.94	53.05
Total	**128**		**30**								
Wt Avg		**0.94**		**0.96**	**48.98**	**0.81**	**0.83**	**44.75**	**0.88**	**0.92**	**46.81**

4.2 Discussion

sEMG and acc were used as the biosignals providing feedback for the design of automated closed-loop DBS system. Since the typical tremor features of PD may vary for different states [13], we trained the algorithms for Action and Posture/Rest trials separately. During the Action state, patients performed a task of extension and flexion of wrist. During Posture state, the patient had to hold their arms out and during Rest trials, the patient placed their arms in a relaxed state. Since during Posture and Rest states, arms of the patient were more or less stationary, we merged the trials in these two states while training for state-specific algorithms. 100% sensitivity was obtained by training the algorithms separately, based on the arm state. An overall higher R_{p} was obtained using LNN-2 for state-specific run compared to states-combined run. Similar better performance of LNN-2 was also observed in trials at DS^{*}. Furthermore, we also compared DT and LNN-2 in offline learning mode, trained and tested on the same set of Action and Posture trials for ET patients. For the same set of test trials, LNN-2 performance metrics are superior to that of DT.

4.2.1 Performance

Performance metrics were chosen to represent how well tremor is predicted. Sensitivity metric gives how well the algorithm performs such that the tremor is predicted before it is actually observed. We may achieve 100% sensitivity if tremor was predicted each time right after stimulation is switched off. Accuracy value expresses performance taking false positives into account. β-ratio evaluates how close to the actual tremor does the algorithm predict its reappearance.

4.2.2 Sensitivity

In case of state-specific run, we were able to achieve 100% sensitivity using LNN-2 for DS^*. This means that there were 0 'misses' and all the predictions were made before the observed reappearance of tremor.

For an on-demand tremor prediction system, it is essential to have 100% sensitivity so that the patient does not feel any discomfort. Sensitivity of LNN-2 is better when run separately for Action and Posture/Rest modes than when the modes are combined together. In case of offline learning comparison of LNN-2 and DT for state-specific training, DT was unable to achieve 100% sensitivity with 1 FN for PD2, whereas, LNN-2 had sensitivity of 100% for all eight PD patients. Both the algorithms achieved 100% sensitivity in case of state-specific training of four ET patients.

4.2.3 Accuracy

An overall accuracy of 83.05% was achieved for 59 trials at DS^* when LNN-2 was separately run for the two states. Accuracy gives the percentage of correctly predicted tremor i.e. $True\ Positive$ when prediction not made too early and $True\ Negative$ when prediction not made in absence of tremor. When trained for Action and Posture/Rest states together, higher number of FP or early predictions were made since voluntary movement may have been mistaken as onset of tremor. It should be mentioned here that the protocol of data collection for "Action" state required patients to perform extension and flexion of the wrist continuously, which inadvertently was periodic in nature. This periodicity of movement and its related frequency range may have characteristics similar to that of tremor, leading to excessive FPs. Further investigation would, therefore, be required in freely-moving patients to better mimic the "Action" state. DT and LNN-2 performed similarly, with respect to the accuracy metric, in case of PD

patients; however, two FP predictions were made by DT in 30 ET test trials, when run in state-specific offline learning mode, giving a lower accuracy for DT compared to that for LNN-2.

4.2.4 β-ratio

The R-ratios given in Table V and Table VIII give a comparison between DT and LNN-2. Table V and Table VIII shows an overall higher R_{p} using LNN-2 than by DT for state-specific training. Compared to trials at all DS, the R-ratios are higher for the trials at DS^* for each patient. For patient PD3, the recordings were done at 40-50 s stimulation periods which may not have included the optimal duration of stimulation for that patient. It should be noted that finding DS^* was not the primary objective of this study; however, it was found during the conduct of this study that R_{o} can be maximized by selecting the right duration of stimulation. This is discussed further in Section 7.2.1. R_{p} of greater than 1 was achieved for patients PD4, PD6 and PD8 at DS^*. This gives DBS "off" time greater than or equal to the duration of stimulation, reducing the amount of stimulation by half or more and increasing the battery life at least by 50%. For 59 trials at DS^*, an average β^* of 0.83 was achieved by LNN-2. A β value close to 1 indicates that the prediction algorithm is able to attain maximum stimulation-free time possible. However, β of 0.97 or higher, is usually not desirable, since there must be some time interval (a few seconds) before DBS starts to suppress tremor. A higher β was obtained by LNN-2 than that by DT for 47 PD test trials as well as for 30 ET trials. A higher percentage of stimulation-free time can be obtained using LNN-2 applied to non-invasive sensors, for PD as well as ET patients. This is essential to maximize the efficacy of closed-loop DBS systems, irrespective of the type of feedback signal.

CHAPTER 5

ON THE NEED FOR ADAPTIVE LEARNING IN ON-DEMAND DEEP BRAIN STIMULATION FOR MOVEMENT DISORDERS

This chapter were published in Nivedita Khobragade, Daniela Tuninetti, Daniel Graupe: On the need for adaptive learning in on-demand Deep Brain Stimulation for Movement Disorders, Engineering in Medicine and Biology Society (EMBC), 40th Annual International Conference of the IEEE, July 2018 ©.

There is an increased interest in designing on-demand DBS systems due to their potential benefits such as reducing amount of stimulation delivered, reduced side-effects as well as reduction in battery power consumption. Studies using approaches of setting single threshold on power of the beta band extracted from LFPs or on tremor power obtained from gyroscope signals have shown to reduce the stimulation delivered, switching on DBS only in presence of symptoms (rigidity and tremor, respectively). Effect of these manually set thresholds have to be studied for chronic use of on-demand system. Other than reliability, an important factor to be considered when selecting the control signal and such thresholds for an on-demand DBS system is robustness over time. Current studies have been carried out over single session without analyzing the chronic implications. The authors of [44] stress that it is essential to shift from acute trials of on-demand systems to their long-term evaluation.

5.1 Training and testing on data from different sessions

Of the recruited patients, one PD patient and one ET patient had two separate data recording sessions at least one week apart. The data collection and feature extraction was same as before. The robustness was then assessed for two machine learning (ML) methods - Decision Tree (DT) and LAMSTAR neural network (LNN) - applied to features extracted from sEMG and accelerometry signals recorded in separate sessions. For both these algorithms, we first carried out training and testing with data of the same session. Next, we trained the algorithm with data of one session and then tested it on that of the other. Since the sEMG sensors and accelerometers are placed externally, this experiment is conducted to test the robustness of such closed-loop systems. The performance metrics are compared for the algorithms when training for tremor prediction was performed on signals from one session and testing on the other session with the results obtained from training and testing on the same session. Performance metrics used for this comparison are defined as previously described in Chapter 3.

5.2 Comparison of performance

Table IX and Table X give the performance metrics of LNN-2 and DT based tremor prediction for patients ET1 and PD6. The number of trials used for training and testing are given as N_{tr} and N_{te}, respectively. The average ratio of observed tremor-free duration without stimulation to the stimulation period before being switched off ($R_{o\ te}$) is listed for all trials in the testing set. The performance metrics include number of True Positives (TP), True Negatives (TN), False Positives (FP) and False Negatives (FN) from which accuracy (A) and sensitivity (S) values were calculated. $R_{p\ te}$ ratio was calculated similar to the $R_{o\ te}$ ratio using predicted tremor-free duration without stimulation for each testing set. When training and testing was performed on the data of the same session (Table IX, sensitivity of

tremor prediction was found to be 100% for both DT and LNN-2. β ratio values are listed for the two algorithms for each session, with higher β for LNN-2. In table Table X, session numbers of the training and testing datasets are given separately. Both DT and LNN-2 showed lower performance when compared to the metrics of same session testing. LNN-2 achieved higher sensitivity compared to DT but 100 % sensitivity was not achieved for all sessions. β was also higher overall for LNN-2 than DT but both the algorithms did not perform as well for different session testing.

TABLE IX. PERFORMANCE METRICS: TRAINING AND TESTING ON DATA FROM THE SAME SESSION

Patient	Session	Trials		$R_{o_{te}}$	Method	Performance metrics				
		N_{tr}	N_{te}			TP, TN, FP, FN	A (%)	S (%)	$R_{p_{te}}$	β
ET1	1	10	3	0.57	DTC	3, 0, 0, 0	100	100	0.4	0.71
					LNN-2	3, 0, 0, 0	100	100	0.53	0.94
ET1	2	31	8	0.93	DTC	4, 2, 2, 0	75	100	0.61	0.66
					LNN-2	6, 2, 0, 0	100	100	0.73	0.78
PD6	1	12	3	2.67	DTC	2, 1, 0, 0	100	100	2.49	0.93
					LNN-2	1, 1, 1, 0	66.67	100	2.3	0.86
PD6	2	11	3	2.87	DTC	3, 0, 0, 0	100	100	2.08	0.73
					LNN-2	3, 0, 0, 0	100	100	2.86	0.99

TABLE X. PERFORMANCE METRICS: TRAINING AND TESTING ON DATA FROM DIFFERENT SESSIONS

Patient	Training session	Trials N_{tr}	Testing session	Trials N_{te}	$R_{o_{te}}$	Method	Performance metrics				
							TP, TN, FP, FN	A (%)	S (%)	$R_{p_{te}}$	β
ET1	1	13	2	39	0.73	DTC	16, 2, 11, 10	46.15	61.54	0.33	0.45
						LNN-2	16, 1, 22, 0	43.56	100	0.3	0.41
ET1	2	39	1	13	1.07	DTC	4, 2, 4, 3	46.15	57.14	0.29	0.27
						LNN-2	6, 0, 6, 1	46.15	85.71	0.49	0.46
PD6	1	15	2	14	2.72	DTC	6, 0, 2, 6	42.85	50	1.5	0.55
						LNN-2	9, 0, 2, 3	64.29	75	1.74	0.64
PD6	2	14	1	15	3.27	DTC	6, 1, 4, 4	46.67	60	1.73	0.53
						LNN-2	9, 1, 5, 0	66.67	100	1.79	0.55

5.3 Need for adaptive learning

Though this comparison of performances is performed for only two patients (2 sessions each), the need for adaptive learning and chronic use assessment is evident. Due to the nature of movement disorders of disease progression and changing symptoms, clinicians evaluate the efficacy of DBS parameter settings at least every three months. Apart from the changes over these longer durations, PD patients have known to experience "on-off" phenomenon due to wear-off of the effect of levodopa medication [45]. While selecting parameters for closed-loop DBS system using any of the available control signal options, the variability of psychological and cognitive state of the patient should also be taken into account. Another factor to be considered for external sensors such as gyroscopes, sEMG and EEG is the effect of small differences in their position on the selected parameters of the closed-loop system for tremor prediction.

We presented here the preliminary results for chronic use of sEMG and accelerometry based on-demand DBS system using two machine learning algorithms. The necessity for an adaptive learning system was observed from the decrease in β-values for different session testing compared to the same session testing. The present on-demand systems designed using power of beta band (extracted from LFPs) or tremor power (obtained from gyroscope signal) require thresholds to be set for the stimulation to be switched on or off. The effect of fluctuations in symptom severity or changes in symptoms over time on the selected threshold needs to be studied. Adaptive systems would update their parameters with the progression of disease. Our main contribution is to show that though both the algorithms predicted tremor with a 100% sensitivity when testing over the same session as that for training, the sensitivity reduces when testing on a different session. It is also found that the ratio of predicted stimulation-off time

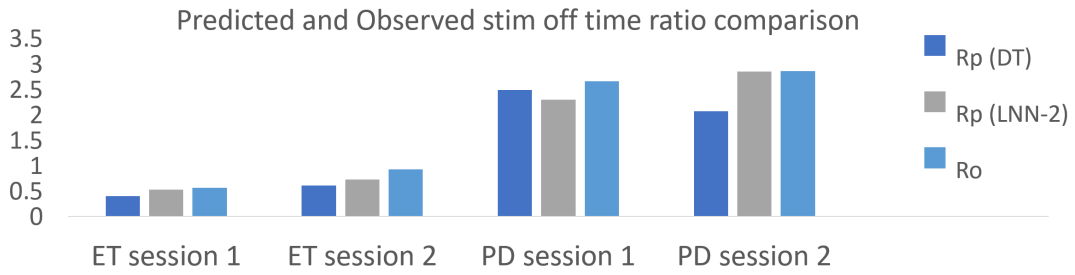

Figure 11. Comparison between predicted and observed R-ratio when training and testing performed on the same session data

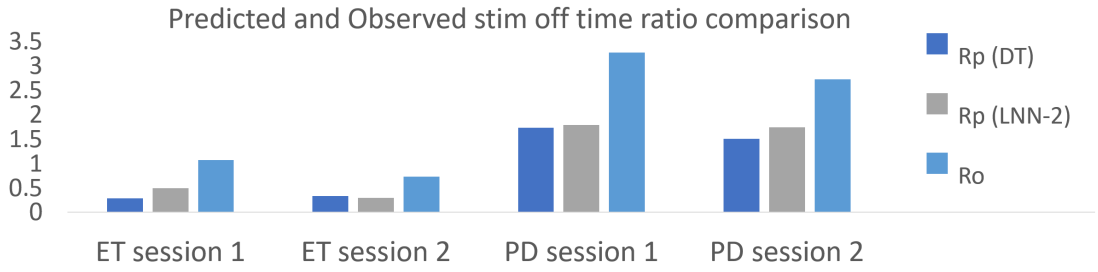

Figure 12. Comparison between predicted and observed R-ratio when training and testing performed on data from different sessions

to observed stimulation-off time reduces when testing on data from the other session. These reduced sensitivity and ratio metrics demonstrate why adaptive learning is essential in on-demand DBS systems. In the future, we intend to develop a tremor-prediction algorithm with online learning capability that would use new information to adapt with changes in symptoms.

CHAPTER 6

DETERMINATION OF DISTINCT PRE-TREMOR INTERVAL FROM SEMG DATA WITHIN TREMOR-FREE-STIMULATION-FREE PERIOD IN PD PATIENTS

Results from this section to be submitted for publication.

While training the machine learning algorithms, a fixed window before observed tremor time point was used for training as the tremor prediction time. The aim of this work to determine the existence of distinct pre-tremor interval from sEMG data was motivated by the observation of a pre-ictal region before epileptic seizure seen in Electroencephalography (EEG) signals. Such pre-ictal intervals do not have a fixed duration before seizure appears as shown by [35]. Here, we show that a specific and distinct Pre-Tremor (PT) interval exists within the No-Stimulation-No-Tremor (NS-NT) period. This was shown using sample entropy and mean frequency features extracted from sEMG data in two tremor-dominant PD patient with high R-ratio. Identifying this PT interval when DBS is off in sEMG signal based features justify the use of sEMG sensors and are important to assess for on-demand predictive control of DBS.

This pre-tremor region is not discernible looking at the signal; however, changes were observed in certain extracted features from the sEMG signal over windows of 5 seconds. The data from one PD6 who had high R-ratio was considered to evaluate the changes in features over time after stimulation is switched off, upto the timepoint where tremor reappeared. In this dataset, one session of PD6 data was used consisting of 10 trials where tremor came back before stimulation was switched on again. Three trials from PD8 were also considered where the R-ratio was high. All the three modes (action,

postural and rest) were analysed. Sample entropy which measures the uncertainty was chosen as one of the features as it can determine increase in regularity in muscle activity associated with appearance of tremor. Mean frequency is also indicative of shift in power which may be related to tremor onset. These two features were evaluated along with rest of the feature set used previously in the machine learning algorithms and were found to be reflective of a pre-tremor region.

6.1 Efficiency operator

The metric used to evaluate these features is described here. Let m, n denote numbers of samples at distances of m, n samples away from observed tremor, where $m > n$. Defining ratio $r(PT, i)$ for all m:

$$r(PT, i; m) = \frac{Nw(PT, i; m)}{m} \tag{6.1}$$

where i is the range, Nw is the number of wins or occurrences in that range, PT stands for pre-tremor

Efficiency E can then be defined as:

$$E = \frac{r(PT, i)}{r(EP, i)} \tag{6.2}$$

where EP denotes the early period before pre-tremor and, prior to first sample considered within the NS-NT period, starting from end of stimulation.

Let:

$$\Delta N(i; m, n) = Nw(PT, i; m)Nw(PT, i; n) \tag{6.3}$$

$$\Delta r(i; m.n) = \frac{\Delta N(i; m, n)}{(m - n)} \tag{6.4}$$

Hence, we define:

$$\Delta E(i) = \frac{\Delta r(i; m, n)}{r(EP, i; m)} \tag{6.5}$$

ΔE denoting an interval of E for samples of data lying at distances between m, n samples away from observed tremor.

6.2 Results

The ranges were set for each of the features in 6 bins based on equal frequency. ΔN and ΔE were calculated over 5 second windows. The six ranges were grouped together to have high, medium, low ranges. Adjacent windows were compared to measure a drop or shift from high to low range for the entropy and the mean frequency which are indicative of tremor reappearance. The results are tabulated for each of the trials over listing the adjacent windows (total 10 second window) where such a drop was observed. There were some drops which were false alarms since they were observed more than 40 seconds before the actual tremor was observed.

TABLE XI. CHANGE IN ENTROPY AND MEAN FREQUENCY

Patient	Trial	delta E		delta N		PT	NSNT
		SaEn	mf	SaEn	mf	start	duration
PD6	post30-1	12.5-22.5, 0-10	12.5-22.5, 0-10	12.5-22.5, 0-10	12.5-22.5, 0-10	22.5	298
	post30-2	40-50, 5-10	40-50, 0-10	40-50, 5-10	45-55, 0-5	40	126
	post30-3	10-25	10-25	10-25	10-25	25	124
	post50-1	5-15	5-15	15-25, 0-5	15-25, 0-5	15	174
	rest30-1	15-25, 0-5	15-25, 0-5	12-22, 0-5	12-22, 0-5	22	107
	rest30-2	0-15	0-15	0-15	0-15	15	185
	rest50-1	0-20	0-20	0-10	0-10	20	31
	act30-3	15-25	15-25	15-25	15-25	25	67
	act30-4	40-50	40-50	40-50	40-50	50	145
	act30-5	15-25, 0-10	15-25, 0-10	15-26, 0-10	15-26, 0-10	25	54
PD8	post30-2	20-30	20-30	20-30	20-30	20	35
	post40-1	20-30	20-30	20-30	20-30	20	132
	rest40-1	16-26	16-26	16-26	16-26	16	69

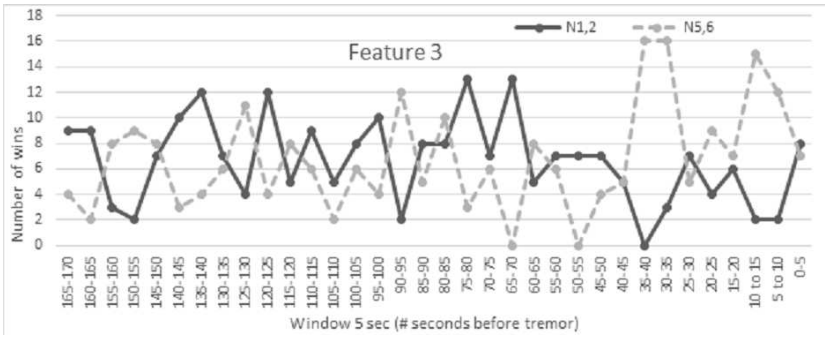

Figure 13. delta N over 5 second windows of mean frequency

Stimulation is restarted at end of the first interval where a decision is made where $\Delta E(N1, N2) > \Delta E(N5, N6)$ Namely where the two lowest ranges dominate the two highest range in both layers F8 and F9 for the last 10 seconds. However, if already prior to 60 seconds into the NS-NT period $\Delta N(N1, N2) > \Delta N(N5, N6)$ where decision is made according to ΔN, since initially ΔE is unreliable due to insufficient data.

Stimulation is to be restarted 10 seconds after estimate of start of PT interval is made.

To take care of the false alarms, mean power in frequency band of 8-16 Hz is used as the 3rd feature. Adding this information can then help reduce the number of early predictions.

6.3 Conclusion

This work shows that there exists a pre-tremor region which can be used for tremor prediction. Only sEMG signal was used to extract three features which show a drop in the ranges during this pre-tremor region. By identifying this region, we provide proof that sEMG can be used as the control signal for

prediction of tremor for design of on-demand DBS system. The data was limited for this study but can be extended to other patients who may be good candidates for on-demand systems and have high R-ratio.

CHAPTER 7

CONCLUSION AND FUTURE WORK

Parts from this chapter to be submitted for publication.

7.1 Conclusion

In this thesis, an automated tremor prediction algorithm has been implemented for the design of closed-loop DBS system in eight PD patients. For each of these individual patients, an optimal duration of stimulation was determined providing the highest stimulation-free period. A comparison was carried out between the performance of combined-states and state-specific runs of LNN-2 algorithm for all durations of stimulation and only the optimal duration of stimulation, specific to each patient. Offline learning algorithms of DT and LNN-2 were also compared for the same eight PD patients and four ET patients. Training was performed on 75-80% of the trials and testing was carried out on the rest. The following conclusions are made from the obtained results:

1. The efficacy of on-demand DBS systems can be maximized by find the optimal duration of stimulation for each patient. In 3 out of 9 patients, R_o of greater than 1 was observed, allowing at least 50% of stimulation-free time. For all patients, an optimal duration of stimulation can be determined which gives the highest stimulation-free time. LNN-2 gave higher R_p for trials at optimal duration stimulation than that for trials at all durations of stimulation.

2. The offline learning comparison showed that LNN-2 performs better than DT for both PD and ET patients. The training and testing trials were separate. Both the machine learning algorithms

performed better when they were trained separately for the different modes of Action and Posture / Rest than when they were trained for the states combined together. In practice, the state-specific tremor predictor would be preceded by another algorithm to classify the state requiring features extracted mainly from accelerometer signal.

3. The need for an adaptive learning algorithm was shown for on-demand systems since the control signals may change with time and the parameters used to predict onset of tremor may not be robust to these changes. By adaptive learning with new data obtained from every day use of the system, the algorithm should be able to monitor these changes and update the parameters accordingly.

4. Sample entropy and mean frequency features were shown to indicate the pre-tremor interval in patient PD6. It is essential to identify the pre-tremor interval for on-demand systems.

5. By using a time-adaptive algorithm, a closed-loop system can be developed that adjusts to the changes in symptom features as the disease progresses. LNN-2 is a feasible option for such an automated system due to its simplicity of implementation. The link weights are updated for the winner neuron of each subword layer in real time. Only when tremor is experienced, the patient needs to manually record the miss of tremor prediction to update the link weights going to output neuron T.

7.2 On-Demand closed-loop DBS in practice

This system would be effective for patients with primary PD symptom of tremor, well-controlled by any type of open-loop DBS. Since tremor is the first symptom to reappear once the stimulation is switched off, other secondary symptoms such as rigidity and bradykinesia would also be taken care

of by this closed-loop system. Feature selection and training need to be carried out for each patient. Since the metrics indicate better performance when the training is done separately for the two states, the algorithm will have to be preceded by a state classifier in practice. IPG programmer should receive a trigger signal from the wearable tremor predictor device via Bluetooth. The external programmer would then communicate the on-off signal to the IPG. This is more convenient in newer IPG programmers which can communicate without direct contact to IPG.

Non-invasive sensors for sEMG plus acc could be stand-alone devices or part of the ubiquitous activity-tracking wearable devices that communicate with the IPG. This closed-loop system would reduce the amount of stimulation being applied to the brain and its related side-effects. It would improve the IPG battery life, reducing the number of battery replacement surgeries, the associated risk of infection and the cumulative cost. It would also be an effective system for rechargeable IPG batteries which have longer lifespan by allowing an increase in the non-charging interval of the battery charging cycle.

7.2.1 Selecting Optimal duration of stimulation

Though this was not the main goal of this study, an important finding has been made during the course of 10 sessions of data collection from nine PD patients. For some patients, tremor did not reappear instantaneously and in some cases, did not reappear even after three minutes of switching of the stimulation. In the on-demand, closed loop DBS systems, stimulation is turned on when onset of tremor is predicted to occur. A predetermined duration of stimulation (DS) is applied, followed by repetition of the process of tremor prediction. DS^* can be selected to maximize, R_o, the ratio of tremor-free period to the stimulation duration [19,46]. Patients who can most benefit from this designed closed-loop system are those for whom tremor does not reappear immediately after discontinuing the

stimulation. Based on these metrics, a clinician should decide whether the patient will benefit from on-demand system and which optimal duration of stimulation would give the maximum percentage of stimulation-free time.

7.2.2 Preventing Paresthesia

Since this on-demand DBS system requires the stimulation to be given in a binary fashion, some patients experience paresthesia or tingling sensation in their hands when stimulation is switched on rapidly after being off for some duration. This sensation due to sudden application of HFS can be overcome by applying a gradually ramping of stimulation onset and offset instead of rapid stimulation [21].

7.2.3 Rechargeables IPGs

Rechargeable IPGs (Medtronic Activa RC, Boston Scientific Vercise) have a longer battery life of 9 to 25 years, requiring less frequent battery replacement surgeries. These need to be recharged every 1-2 weeks for 3-4 hours. Such systems may also benefit from a closed-loop DBS by improving the battery charging cycle. By stimulating on-demand, the number of days without recharging can be increased.

7.2.4 Continuous learning

From the metrics discussed in results section, LNN-2 showed better overall performance compared to DT. An important advantage of LNN-2, which makes it a superior prediction algorithm than DT, is its ability to continuously adapt with newer information. In case of DT, the training once completed, the thresholds remain unchanged over time, irrespective of the changes in PD symptoms. Incremental DT, which is an online learning method, requires the Classification and Regression Tree (CART) algorithm to be modified to evaluate the change in impurity at each node that the new instance traversed and find

the new optimal split for the given change in impurity [47]. However, LNN-2 can continue learning online with every new input feature set, continually adapting to the disease progression, without any modification to the current architecture. The system can be set up such that, the link-weights to no-tremor (NT) neuron are rewarded as long as tremor is not observed. If the patient experiences tremor, a manual button tap would indicate occurrence of tremor so that "punishment" is given to the NT neuron link-weights and tremor (T) neuron link-weights are rewarded.

7.3 Future work

7.3.1 sEMG and acc signals recorded from free-moving patients

The current data collection protocol for all eight PD patients and four ET patients required the patients to carry out one of the three tasks in each trial: Action where the wrist would be extended or flexed, Posture where the hands are extended out horizontally or Rest where the limb remain stationary with no effort exerted on the sEMG muscle source. Action task performed by the patients is repetitive and periodic in nature. Such controlled environment does not completely reflect the activities of free-moving patients. It is, therefore, essential to also collect and analyse data during daily activities of the patients in their natural environment.

7.3.2 Extending to other disorders

A similar analysis has to be carried out for ET data from the second recording set-up. Online learning approach, LNN-2, has to be implemented for all ET patients (four from first set-up and two from second set-up) following the state-classifier algorithm. An analysis will also be carried out on sEMG+acc data recorded from a non-tremor PD patient and from open-access wearable data of NTD PD patients to assess if bradykinesia can be tracked for on-demand DBS systems.

APPENDICES

1. Permission to reuse in Thesis/ dissertation from **Wiley publications** *Daniel Graupe, Nivedita Khobragade, Daniela Tuninetti, Ishita Basu, Konstantin Slavin, Leo Verhagen Metman: Who may benefit from on-demand control of DBS: a non-invasive Parkinson patients evaluation, Neuromodulation: Technology at the Neural Interface, 2018*

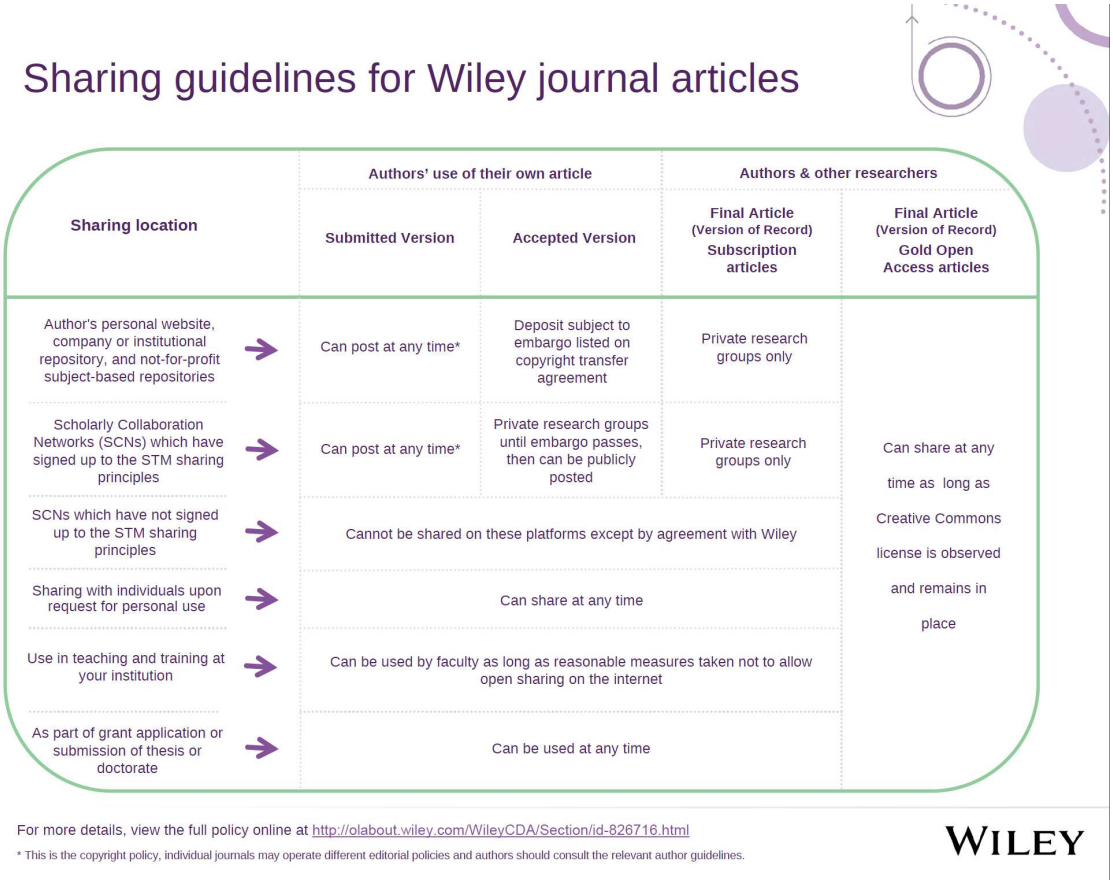

Sharing guidelines for Wiley journal articles

Sharing location	Authors' use of their own article		Authors & other researchers	
	Submitted Version	Accepted Version	Final Article (Version of Record) Subscription articles	Final Article (Version of Record) Gold Open Access articles
Author's personal website, company or institutional repository, and not-for-profit subject-based repositories →	Can post at any time*	Deposit subject to embargo listed on copyright transfer agreement	Private research groups only	Can share at any time as long as Creative Commons license is observed and remains in place
Scholarly Collaboration Networks (SCNs) which have signed up to the STM sharing principles →	Can post at any time*	Private research groups until embargo passes, then can be publicly posted	Private research groups only	
SCNs which have not signed up to the STM sharing principles →	Cannot be shared on these platforms except by agreement with Wiley			
Sharing with individuals upon request for personal use →	Can share at any time			
Use in teaching and training at your institution →	Can be used by faculty as long as reasonable measures taken not to allow open sharing on the internet			
As part of grant application or submission of thesis or doctorate →	Can be used at any time			

For more details, view the full policy online at http://olabout.wiley.com/WileyCDA/Section/id-826716.html

* This is the copyright policy, individual journals may operate different editorial policies and authors should consult the relevant author guidelines.

WILEY

This Agreement between ("You") and John Wiley and Sons ("John Wiley and Sons") consists of your license details and the terms and conditions provided by John Wiley and Sons and Copyright Clearance Center.

License Number	4642590681572
License date	Aug 05, 2019
Licensed Content Publisher	John Wiley and Sons
Licensed Content Publication	NEUROMODULATION: TECHNOLOGY AT THE NEURAL INTERFACE
Licensed Content Title	Who May Benefit From On-Demand Control of Deep Brain Stimulation? Noninvasive Evaluation of Parkinson Patients
Licensed Content Author	Daniel Graupe, Nivedita Khobragade, Daniela Tuninetti, et al
Licensed Content Date	Jan 18, 2018
Licensed Content Volume	21
Licensed Content Issue	6
Licensed Content Pages	5
Type of use	Dissertation/Thesis
Requestor type	Author of this Wiley article
Format	Electronic
Portion	Text extract
Number of Pages	3
Will you be translating?	No
Title of your thesis / dissertation	Design of On-demand DBS in Movement Disorders using Machine Learning and the Need for Adaptive Learning
Expected completion date	Aug 2019
Expected size (number of pages)	4
Requestor Location	SAN MATEO, CA 94403 United States
Publisher Tax ID	EU826007151
Total	0.00 USD
Terms and Conditions	

Terms and Conditions

- The materials you have requested permission to reproduce or reuse (the ”Wiley Materials”) are protected by copyright.
- You are hereby granted a personal, non-exclusive, non-sub licensable (on a standalone basis), non-transferable, worldwide, limited license to reproduce the Wiley Materials for the purpose specified in the licensing process. This license, and any CONTENT (PDF or image file) purchased as part of your order, is for a one-time use only and limited to any maximum distribution number specified in the license. The first instance of republication or reuse granted by this license must be completed within two years of the date of the grant of this license (although copies prepared before the end date may be distributed thereafter). The Wiley Materials shall not be used in any other manner or for any other purpose, beyond what is granted in the license. Permission is granted subject to an appropriate acknowledgement given to the author, title of the material/book/journal and the publisher. You shall also duplicate the copyright notice that appears in the Wiley publication in your use of the Wiley Material. Permission is also granted on the understanding that nowhere in the text is a previously published source acknowledged for all or part of this Wiley Material. Any third party content is expressly excluded from this permission.
- With respect to the Wiley Materials, all rights are reserved. Except as expressly granted by the terms of the license, no part of the Wiley Materials may be copied, modified, adapted (except for minor reformatting required by the new Publication), translated, reproduced, transferred or distributed, in any form or by any means, and no derivative works may be made based on the Wiley Materials without the prior permission of the respective copyright owner.For STM Signatory Pub-

lishers clearing permission under the terms of the STM Permissions Guidelines only, the terms of the license are extended to include subsequent editions and for editions in other languages, provided such editions are for the work as a whole in situ and does not involve the separate exploitation of the permitted figures or extracts, You may not alter, remove or suppress in any manner any copyright, trademark or other notices displayed by the Wiley Materials. You may not license, rent, sell, loan, lease, pledge, offer as security, transfer or assign the Wiley Materials on a stand-alone basis, or any of the rights granted to you hereunder to any other person.

- The Wiley Materials and all of the intellectual property rights therein shall at all times remain the exclusive property of John Wiley & Sons Inc, the Wiley Companies, or their respective licensors, and your interest therein is only that of having possession of and the right to reproduce the Wiley Materials pursuant to Section 2 herein during the continuance of this Agreement. You agree that you own no right, title or interest in or to the Wiley Materials or any of the intellectual property rights therein. You shall have no rights hereunder other than the license as provided for above in Section 2. No right, license or interest to any trademark, trade name, service mark or other branding (”Marks”) of WILEY or its licensors is granted hereunder, and you agree that you shall not assert any such right, license or interest with respect thereto
- NEITHER WILEY NOR ITS LICENSORS MAKES ANY WARRANTY OR REPRESENTATION OF ANY KIND TO YOU OR ANY THIRD PARTY, EXPRESS, IMPLIED OR STATUTORY, WITH RESPECT TO THE MATERIALS OR THE ACCURACY OF ANY INFORMATION CONTAINED IN THE MATERIALS, INCLUDING, WITHOUT LIMITATION, ANY IMPLIED WARRANTY OF MERCHANTABILITY, ACCURACY, SATISFACTORY QUAL-

ITY, FITNESS FOR A PARTICULAR PURPOSE, USABILITY, INTEGRATION OR NON-INFRINGEMENT AND ALL SUCH WARRANTIES ARE HEREBY EXCLUDED BY WILEY AND ITS LICENSORS AND WAIVED BY YOU.

- WILEY shall have the right to terminate this Agreement immediately upon breach of this Agreement by you.
- You shall indemnify, defend and hold harmless WILEY, its Licensors and their respective directors, officers, agents and employees, from and against any actual or threatened claims, demands, causes of action or proceedings arising from any breach of this Agreement by you.
- IN NO EVENT SHALL WILEY OR ITS LICENSORS BE LIABLE TO YOU OR ANY OTHER PARTY OR ANY OTHER PERSON OR ENTITY FOR ANY SPECIAL, CONSEQUENTIAL, INCIDENTAL, INDIRECT, EXEMPLARY OR PUNITIVE DAMAGES, HOWEVER CAUSED, ARISING OUT OF OR IN CONNECTION WITH THE DOWNLOADING, PROVISIONING, VIEWING OR USE OF THE MATERIALS REGARDLESS OF THE FORM OF ACTION, WHETHER FOR BREACH OF CONTRACT, BREACH OF WARRANTY, TORT, NEGLIGENCE, INFRINGEMENT OR OTHERWISE (INCLUDING, WITHOUT LIMITATION, DAMAGES BASED ON LOSS OF PROFITS, DATA, FILES, USE, BUSINESS OPPORTUNITY OR CLAIMS OF THIRD PARTIES), AND WHETHER OR NOT THE PARTY HAS BEEN ADVISED OF THE POSSIBILITY OF SUCH DAMAGES. THIS LIMITATION SHALL APPLY NOTWITHSTANDING ANY FAILURE OF ESSENTIAL PURPOSE OF ANY LIMITED REMEDY PROVIDED HEREIN.

- Should any provision of this Agreement be held by a court of competent jurisdiction to be illegal, invalid, or unenforceable, that provision shall be deemed amended to achieve as nearly as possible the same economic effect as the original provision, and the legality, validity and enforceability of the remaining provisions of this Agreement shall not be affected or impaired thereby.
- The failure of either party to enforce any term or condition of this Agreement shall not constitute a waiver of either party's right to enforce each and every term and condition of this Agreement. No breach under this agreement shall be deemed waived or excused by either party unless such waiver or consent is in writing signed by the party granting such waiver or consent. The waiver by or consent of a party to a breach of any provision of this Agreement shall not operate or be construed as a waiver of or consent to any other or subsequent breach by such other party.
- This Agreement may not be assigned (including by operation of law or otherwise) by you without WILEY's prior written consent.
- Any fee required for this permission shall be non-refundable after thirty (30) days from receipt by the CCC.
- These terms and conditions together with CCC's Billing and Payment terms and conditions (which are incorporated herein) form the entire agreement between you and WILEY concerning this licensing transaction and (in the absence of fraud) supersedes all prior agreements and representations of the parties, oral or written. This Agreement may not be amended except in writing signed by both parties. This Agreement shall be binding upon and inure to the benefit of the parties' successors, legal representatives, and authorized assigns.

- In the event of any conflict between your obligations established by these terms and conditions and those established by CCC's Billing and Payment terms and conditions, these terms and conditions shall prevail.
- WILEY expressly reserves all rights not specifically granted in the combination of (i) the license details provided by you and accepted in the course of this licensing transaction, (ii) these terms and conditions and (iii) CCC's Billing and Payment terms and conditions.
- This Agreement will be void if the Type of Use, Format, Circulation, or Requestor Type was misrepresented during the licensing process.
- This Agreement shall be governed by and construed in accordance with the laws of the State of New York, USA, without regards to such state's conflict of law rules. Any legal action, suit or proceeding arising out of or relating to these Terms and Conditions or the breach thereof shall be instituted in a court of competent jurisdiction in New York County in the State of New York in the United States of America and each party hereby consents and submits to the personal jurisdiction of such court, waives any objection to venue in such court and consents to service of process by registered or certified mail, return receipt requested, at the last known address of such party.

2. Permission to reuse in Thesis/ dissertation from **IEEE EMBC proceedings** *Nivedita Khobragade, Daniel Graupe, Daniela Tuninetti: Towards fully automated closed-loop Deep Brain Stimulation in Parkinson's disease patients: A LAMSTAR-based tremor predictor, Engineering in Medicine and Biology Society (EMBC), 37th Annual International Conference of the IEEE, August 2015* and *Nivedita Khobragade, Daniela Tuninetti, Daniel Graupe: On the need for adaptive learning in on-demand Deep Brain Stimulation for Movement Disorders, Engineering in Medicine and Biology Society (EMBC), 40th Annual International Conference of the IEEE, July 2018*

Thesis / Dissertation Reuse

The IEEE does not require individuals working on a thesis to obtain a formal reuse license, however, you may print out this statement to be used as a permission grant:

Requirements to be followed when using any portion (e.g., figure, graph, table, or textual material) of an IEEE copyrighted paper in a thesis:

1) In the case of textual material (e.g., using short quotes or referring to the work within these papers) users must give full credit to the original source (author, paper, publication) followed by the IEEE copyright line ©2011 IEEE.

2) In the case of illustrations or tabular material, we require that the copyright line ©[Year of original publication] IEEE appear prominently with each reprinted figure and/or table.

3) If a substantial portion of the original paper is to be used, and if you are not the senior author, also obtain the senior author's approval.

Requirements to be followed when using an entire IEEE copyrighted paper in a thesis:

1) The following IEEE copyright/ credit notice should be placed prominently in the references: ©[year of original publication] IEEE. Reprinted, with permission, from [author names, paper title, IEEE publication title, and month/year of publication]

2) Only the accepted version of an IEEE copyrighted paper can be used when posting the paper or your thesis on-line.

3) In placing the thesis on the author's university website, please display the following message in a prominent place on the website: In reference to IEEE copyrighted material which is used with permission in this thesis, the IEEE does not endorse any of [university/educational entity's name goes here]'s products or services. Internal or personal use of this material is permitted. If interested in reprinting/republishing IEEE copyrighted material for advertising or promotional purposes or for creating new collective works for resale or redistribution, to learn how to obtain a License from RightsLink, please go to:

$http://www.ieee.org/publications\_standards/publications/rights/rights\_link.html$.

If applicable, University Microfilms and/or ProQuest Library, or the Archives of Canada may supply single copies of the dissertation.

CITED LITERATURE

1. A. L. Benabid, P. Pollak, A. Louveau, S. Henry, and J. de Rougemont. Combined (thalamotomy and stimulation) stereotactic surgery of the vim thalamic nucleus for bilateral parkinson disease. Journal of Applied Neurophysiology, 50:344–346, 1987.

2. A. Lozano and N. Lipsman. Probing and regulating dysfunctional circuits using deep brain stimulation. Neuron, 77:406–424, 2013.

3. Nathan C. Rowland, Francesco Sammartino, and Andres M. Lozano. Advances in surgery for movement disorders. Movement Disorders, 32(1):5–10, 2017.

4. Adam O Hebb, Jun Jason Zhang, Mohammad H Mahoor, Christos Tsiokos, Charles Matlack, Howard Jay Chizeck, and Nader Pouratian. Creating the feedback loop: closed-loop neurostimulation. Neurosurgery Clinics, 25(1):187–204, 2014.

5. Marwan Hariz. Deep brain stimulation: new techniques. Parkinsonism & related disorders, 20:S192–S196, 2014.

6. A. Priori. Technology for deep brain stimulation at a gallop. Movement Disorders, 30:1206–1212, 2015.

7. B. Rosin, M. Slovik, R. Mitelman, M. Rivlin-Etzion, S. N. Haber, Z. Israel, E. Vaadia, and H. Bergman. Closed-loop deep brain stimulation is superior in ameliorating parkinsonism. Neuron, 72:370–384, 2011.

8. M Beudel and P Brown. Adaptive deep brain stimulation in parkinson's disease. Parkinsonism & related disorders, 22:S123–S126, 2016.

9. A. Fytagoridis, T. Heard, J. Samuelsson, P. Zsigmond, E. Jiltsova, S. Skyrman, T. Skoglund, T. Coyne, P. Silburn, and P. Blomstedt. Surgical replacement of implantable pulse generators in deep brain stimulation: Adverse events and risk factors in a multicenter cohort. Stereotactical and Functional Neurosurgery, 94:235–239, 2016.

10. A. Ascherio and M. Schwarzschild. The epidemiology of parkinson's disease: risk factors and prevention. The Lancet Neurology, 15:1257–1272, 2016.

11. R. Helmich, M. Hallett, G. Deuschl, I. Toni, and B. Bloem. Cerebral causes and consequences of parkinsonian resting tremor. Brain, 135:3206–3226, 2012.

12. J. Jankovic and E. Tolosa. Parkinsons disease and movement disorders. Lippincott Williams and Wilkins Philadelphia, 2007.

13. G. Deuschl, P. Bain, and M. Brin. Consensus statement of the movement disorder society on tremor. Movement Disorders, 13:2–23, 1998.

14. E. Tripoliti, L. Strong, T. Foltynie, L. Zrinzo, J. Candelario, M. Hariz, and P. Limousin. Treatment of dysarthria following subthalamic nucleus deep brain stimulation for parkinson's disease. Movement Disorders, 26:2434–2436, 2011.

15. Z. Zheng, Y. Li, J. Li, Y. Zhang, X. Zhang, and P. Zhuang. Stimulation-induced dyskinesia in the early stage after subthalamic deep brain stimulation. Stereotactic Functional Neurosurgery, 88:29–34, 2010.

16. S. Little, A. Pogosyan, S. Neal, B. Zavala, L. Zrinzo, M. Hariz, T. Foltynie, P. Limousin, K. Ashkan, J. FitzGerald, A. L. Green, T. Z. Aziz, and P. Brown. Adaptive deep brain stimulation in advanced parkinson disease. Annals of Neurology, 74:449–457, 2013.

17. J. Benito-Leon and E. Louid. Essential tremor: emerging views of a common disorder. Nature Reviews Neurology, 2:666–678, 2006.

18. H. Cagnan, J. Brittain, S. Little, T. Foltynie, P. Limousin, L. Zrinzo, M. Hariz, C. Joint, J. Fitzgerald, A. Green, T. Aziz, and P. Brown. Phase dependent modulation of tremor amplitude in essential tremor through thalamic stimulation. Brain, 136:3062–3075, 2013.

19. D. Graupe, I. Basu, D. Tuninetti, P. Vannemreddy, and K. Slavin. Adaptively controlling deep brain stimulation in essential tremor patient via surface electromyography. Neurological Research, 32:899–904, 2010.

20. J. Herron, M. Thompson, T. Brown, H. Chizeck, J. Ojemann, and A. Ko. Cortical brain computer interface for closed-loop deep brain stimulation. IEEE transactions on Neural Systems and Rehabilitation Engineering, PP, 2017.

21. M. Beudel and P. Brown. Adaptive deep brain stimulation in parkinsons disease. Parkinsonism and Related Disorders, 22:S123–S126, 2016.

22. I. Basu, D. Graupe, D. Tuninetti, P. Shukla, K. V. Slavin, L. Verhagen Metman, and D. M. Corcos. Pathological tremor prediction using surface electromyogram and acceleration: potential use in on-off dem and driven deep brain stimulator design. Journal of Neural Engineering, 10:036019, 2013.

23. Mahsa Malekmohammadi, Jeffrey Herron, Anca Velisar, Zack Blumenfeld, Megan H. Trager, Howard Jay Chizeck, and Helen Bront-Stewart. Kinematic adaptive deep brain stimulation for resting tremor in parkinson's disease. Movement Disorders, 31(3):426–428, 2016.

24. F. Santos, R. Costa, and F. Tecuapetla. Stimulation on demand: Closing the loop on deep brain stimulation. Neuron, 72, 2011.

25. M. Rosa, M. Arlotti, G. Ardolino, F. Cogiamanian, S. Marceglia, A. Di Fonzo, F. Cortese, P. Rampini, and A. Priori. Adaptive deep brain stimulation in a freely moving parkinsonian patient. Movement Disorders, 30:1003–1005, 2015.

26. P. Temperli, J. Ghika, J. G. Villemure, P. R. Burkhard, J. Bogousslavsky, and F. J. Vingerhoets. How do parkinsonian signs return after discontinuation of subthalamic dbs? Neurology, 60:78–81, 2003.

27. Shyamal Patel, Hyung Park, Paolo Bonato, Leighton Chan, and Mary Rodgers. A review of wearable sensors and systems with application in rehabilitation. Journal of NeuroEngineering and Rehabilitation, 9(1):21, 2012.

28. Peter J. Grahn, Grant W. Mallory, Obaid U. Khurram, B. Michael Berry, Jan T. Hachmann, Allan J. Bieber, Kevin E. Bennet, Hoon-Ki Min, Su-Youne Chang, Kendall H. Lee, and J. L. Lujan. A neurochemical closed-loop controller for deep brain stimulation: toward individualized smart neuromodulation therapies. Frontiers in Neuroscience, 8:169, 2014.

29. R. Carron, A. Chaillet, A. Filipchul, W. Pasillas-Lepine, and C. Hammond. Closing the loop of deep brain stimulation. Frontiers in Systems Neuroscience, 7:112, 2013.

30. E. Opri, J. Shute, R. Molina, K. Foote, M. Okun, and A. Gunduz. Closing the loop in deep brain stimulation: A responsive treatment for essential tremor (s27.005). Neurology, 86, 2016.

31. Takamitsu Yamamoto, Yoichi Katayama, Junichi Ushiba, Hiroko Yoshino, Toshiki Obuchi, Kazutaka Kobayashi, Hideki Oshima, and Chikashi Fukaya. On-demand control system for deep brain stimulation for treatment of intention tremor. Neuromodulation: Technology at the Neural Interface, 16(3):230–235, 2013.

32. P. Shukla, I. Basu, D. Graupe, D. Tuninetti, and K. V. Slavin. A neural network-based design of an on-off adaptive control for deep brain stimulation in movement disorders. In Engineering in Medicine and Biology Society (EMBC), 2012 Annual International Conference of the IEEE, pages 4140–4143, 2012.

33. Pitamber Shukla. Machine Learning Technique Based Closed-loop Deep Brain Stimulation Controller Design. PhD thesis, University of Illinois at Chicago, 2015.

34. N. Khobragade, D. Graupe, and D. Tuninetti. Towards fully automated closed-loop deep brain stimulation in parkinson's disease patients: A lamstar-based tremor predictor. In Engineering in Medicine and Biology Society (EMBC), 2015 37th Annual International Conference of the IEEE, pages 2616–2619, 2015.

35. V. Nigam and D. Graupe. A neural-network-based detection of epilepsy. Neurological Research, 26:55–60, 2004.

36. J. A. Waxman, D. Graupe, and D. W. Carley. Automated prediction of apnea and hypopnea,using a lamstar artificial neural network. Am J Respir Crit Care Med., 181(7):727–723, 2010.

37. N. Schneider and D. Graupe. A modified lamstar neural network and its applications. International Journal of Neural Systems, 18:331–337, 2008.

38. D. Graupe. Deep Learning Neural Networks: Design and Case Studies. World Scientific, 2016.

39. Dario Farina, Luigi Fattorini, Francesco Felici, and Giancarlo Filligoi. Nonlinear surface emg analysis to detect changes of motor unit conduction velocity and synchronization. Journal of Applied Physiology, 93:1753–1763, 2002.

40. GianCarlo Filligoi and Francesco Felici. Detection of hidden rhythms in surface emg signals with a non-linear time-series tool. Medical Engineering and Physics, 21:439–448, 1999.

41. C L. Webber Jr and J P. Zbilut. Recurrence quantification analysis of nonlinear dynamical systems. Tutorials in contemporary nonlinear methods for the behavioral sciences, pages 26–94, 2005.

42. Usama Fayyad and Keki Irani. Multi-interval discretization of continuous-valued attributes for classication learning. In Proceedings of Thirteenth International Joint Conference on Uncertainty in Artificial Intelligence, pages 1022–1027, 1993.

43. Farzan Farnia and David Tse. A minimax approach to supervised learning. In Advances in Neural Information Processing Systems, pages 4240–4248, 2016.

44. Adolfo Ramirez-Zamora, James J Giordano, Aysegul Gunduz, Peter Brown, Justin Sanchez, Kelly Douglas Foote, Leonardo Almeida, Philip Starr, Helen M Bronte-Stewart, Cameron McIntyre, et al. Evolving applications, technological challenges and future opportunities in neuromodulation: Proceedings of the fifth annual deep brain stimulation think tank. Frontiers in Neuroscience, 11:734, 2017.

45. Roongroj Bhidayasiri and Daniel Tarsy. Parkinsons disease:on-off phenomenon. In Movement Disorders: A Video Atlas, pages 14–15. Springer, 2012.

46. D. Graupe, N. Khobragade, D. Tuninetti, K. Slavin, L. Verhagen, I. Basu, and A. Rabie. Patient data concerning emg-based on-demand predictive control of dbs for parkinson patients and significance. European Journal of Translational Myology, 25, 2015.

47. S. Crawford. Extensions to the cart algorithm. Int. Journal of Man-Machine Studies, 31:197–217, 1989.

VITA

NAME: Nivedita Khobragade

EDUCATION: B.E., Electronics Engineering, Veermata Jijabai Technological Institute, Mumbai, India

M.S., Biomedical Engineering, University of Texas at Arlington, Arlington, Texas

Ph.D.,Electrical & Computer Engineering, University of Illinois at Chicago, Illinois

RESEARCH: Research Assistant in Biomedical Signal Processing Lab, Department of Electrical & Computer Engineering, University of Illinois at Chicago, 2013–2015

Research Assistant in Regenerative Neurobiology Lab, Department of Biomedical Engineering, University of Texas at Arlington, 2010–2011

TEACHING: Teaching Assistant in department of Electrical & Computer Engineering, University of Illinois at Chicago, 2015–2018

Teaching Assistant in department of Biomedical Engineering, University of Texas at Arlington, 2011

PROFESSIONAL EXPERIENCE:

Physiologic Algorithms Intern at Proteus Digital Health, Redwood City, CA, Summer 2016

Software Engineer at HSBC Global Technology, Pune, India, 2007–2009

SCHOLARSHIPS and MEMBERSHIPS:

Robert Eberhart scholarship, University of Texas at Arlington, 2010-11.

Student member of Tau Beta Pi (Engineering Honor Society)

Student member of IEEE engineering in Medicine and Biology (EMB) society

SKILLS

Proficient in Python, MatLab and C,
Experience in DB2, SQL, DataStage,
Working knowledge of SAS, R,
Expertise in In-vivo and surface Electrophysiology,
Immunohistochemistry, Confocal and Fluorescence microscopy

PUBLICATIONS:

Daniel Graupe, Nivedita Khobragade, Daniela Tuninetti, Ishita Basu, Konstantin Slavin, Leo Verhagen Metman: **Who may benefit from on-demand control of DBS: a non-invasive Parkinson patients evaluation**, Neuromodulation: Technology at the Neural Interface, 2018

Nivedita Khobragade: **Micromotion and scarring do not contribute to Failure of Regenerative Peripheral Neural Interfacing**, Masters thesis, University of Texas at Arlington, 2012

Nivedita Khobragade, Daniela Tuninetti, Daniel Graupe, Leo Verhagen Metman, Konstantin Slavin, Ishita Basu: **On-demand Control of DBS using Non-invasive EMG sensors in Movement Disorders**, to be submitted

CONFERENCE PROCEEDINGS AND POSTERS:

Nivedita Khobragade, Daniela Tuninetti, Daniel Graupe: **On the need for adaptive learning in on-demand Deep Brain Stimulation for Movement Disorders**, Engineering in Medicine and Biology Society (EMBC), 40th Annual International Conference of the IEEE, July 2018

Nivedita Khobragade, Chirag Agarwal: **Multi-class segmentation of neuronal electron microscopy images using deep learning**, SPIE Medical Imaging, March 2018

Nivedita Khobragade, Daniel Graupe, Daniela Tuninetti: **Towards fully automated closed-loop Deep Brain Stimulation in Parkinson's disease patients: A LAMSTAR-based tremor predictor**, Engineering in Medicine and Biology Society (EMBC), 37th Annual International Conference of the IEEE, August 2015

Daniel Graupe, Nivedita Khobragade, Daniel Tuninetti, Konstantin V Slavin, Leonard Verhagen Metman, and Ahmed Rabie: **Patient Data Concerning EMG-Based On-Demand Predictive Control of DBS for Parkinson Patients and Significance**, European Journal of Translational Myology, March 2015

Nivedita Khobragade, Vidhi Desai, Jennifer Seifert, Poorva Abhyankar, Young Kim, An Nguyen, Mario Romero-Ortega: **Neural Activity Decay in Regenerative Peripheral Interfaces Correlates with Axonal Remyelination**, Society for Neuroscience, 2011

Vidhi Desai, Collins Watson, Nilanjana Dutta, Nivedita Khobragade, An Nguyen, Jennifer Seifert, Mario Romero-Ortega: **Specific single unit neural activity recorded from regenerative peripheral nerve interface corresponding with movement and response to mechanical and thermal stimulation**, Society for Neuroscience, 2011

Jennifer Seifert, Collins Watson, Stephen Kunkel, Vidhi Desai, Nivedita Khobragade, Nilanjana Dutta, Young-Tae Kim, Mario Romero-Ortega: **The stability of a regenerative multielectrode interface is unaffected by either normal or excessive cyclical limb stretching**, Society for Neuroscience, 2011

Vidhi Desai, Sarita Bhetwal, Nivedita Khobragade, Collins Watson, Nilanjana Dutta, Jennifer Seifert, Mario Romero-Ortega: **Transcription factor analysis indicates that limb stretching does not alter Regenerative multielectrode interfacing of peripheral nerves**, Neural Interfaces Conference, 2012

Vidhi Desai, Sarita Bhetwal, Nivedita Khobragade, Collins Watson, An Nguyen, Jennifer Seifert, Mario Romero-Ortega: **Normal ATF-3 and cJUN expression in sensory neurons of peripheral nerve interfaced animals despite nerve stretching**, Society for Neuroscience, 2012